IDM UID
ATYFD5

VERSION CREATED ON / VERSION / STATUS
05 Jun 2024 / 1.0 / Approved

EXTERNAL REFERENCE / VERSION
80693e6b / r1.0

DA DOCUMENT DELIVERABLE

Sub-System or Equipment Design Description

55.GA UWAVS Technical Design Description of Back End Optics and Cameras (304243-R00028 A.4)

Contains a detailed technical description for the UWAVS Back-end Optical and Camera assembly with its subassemblies and components. This document is referenced in the DDD. For reviewers and approver, please refer to DPP template - https://user.iter.org/?uid=RZJ4LM

Approval Process			
	Name	*Action*	*Affiliation*
Signatory	**Bhatia R.**	**05 Jun 2024:signed**	
Co-signatories			
Reviewers	**Kocan M.** **Martin V.** **Ye C.**	**12 Jul 2024:recommended** **18 Jun 2024:recommended** **13 Jun 2024:recommended**	**IO/DG/CP/DIAG/EVD** **IO/DG/CP/DIAG/EVD** **IO/DG/SQD/QMD/QA**
Approver	**Reichle R.**	**19 Jul 2024:approved**	**IO/DG/CP/DIAG/EVD**
Information Protection Level: Non-Public - Unclassified *RO: Martin Vincent*			
Read Access	**LG: DA DIAG PA TRO 55.C5, 55.E5, 55.EB, 55.F1.AU/BU/CU, 55.F2, 55.GA, AD: IO_Director-General, AD: External Management Advisory Board, AD: IDM_Controller, AD: Auditors, project administrator, RO, LG: I&C_Design_Survey, LG: USDA_PA_PT_Common, LG: USDA_55.GA_PT, LG: IO TRO GA/UB/UE, LG: IO PA PT Diag ...**		

Change Log			
55.GA UWAVS Technical Design Description of Back End Optics and Cameras (304243-R00028 A.4) (ATYFD5)			
Version	***Latest Status***	***Issue Date***	***Description of Change***
v0.0	In Work	20 Mar 2024	
v1.0	Approved	05 Jun 2024	Initial Issue

Preliminary

CLASSIFICATION	EDRM UID	ICP Number
Unclassified Non-Sensitive	**80693e6b - 1.0**	**ITER_D_ATYFD5**
EXTERNAL REFERENCE	VERSION CREATED ON / STATUS	
304243-R00028 Rev. A	**05 Jun 2024 / Approved**	
PA DESIGN DOCUMENT TYPE	DRAWING NUMBER	DRAWING REV
System Design Description (DD)		
PA/TA NUMBER(s)		iDOCS UID
5.5.P3.US.01 - VIR/UP11/UP14		

55.GA UWAVS Technical Design Description of Back End Optics and Cameras (304243-R00028 A)

Abstract or description:

Contains a detailed technical description for the UWAVS Back-end Optical and Camera assembly with its subassemblies and components. This document is referenced in the DDD.

Workflow Role	Name	Date	Status
Signatory	Smith, Mark	31 May 2024	Signed
Reviewer	Temple, Patrick	05 Jun 2024	Recommended
Approver	Bhatia, Ravinder	05 Jun 2024	Approved

DISCLAIMER: UNCONTROLLED WHEN PRINTED – PLEASE CHECK THE STATUS OF THE DOCUMENT IN EDRM

Preliminary

Change Log

Version	State	Date	Version Change Description
v1.0	Approved	05 Jun 2024	

DISCLAIMER: UNCONTROLLED WHEN PRINTED – PLEASE CHECK THE STATUS OF THE DOCUMENT IN EDRM

PRINCETON PLASMA PHYSICS LABORATORY

ITER UPPER WIDE ANGLE VIEWING SYSTEM PROJECT

55.GA UWAVS TECHNICAL DESIGN DESCRIPTION FOR BACK-END OPTICS AND CAMERAS

Sponsored by Oak Ridge National Laboratory
c/o Princeton Plasma Physics Laboratory

Under Subcontract No: S013437

Prepared by General Atomics

304243-R00028
Revision A
GA Project 30424

PPPL APPROVAL

VERSION	Date	Signatory	QA Engineer	SE	External ITER Reviewer	Approver
1.0	5/28/2024	Mark Smith	Patrick Temple	Pete Dugan	N/A	Ravinder Bhatia
		SEE EDRM	SEE EDRM	Notification	N/A	SEE EDRM

304243-R00028
Revision A

ITER UPPER WIDE ANGLE VIEWING SYSTEM PROJECT

55.GA UWAVS TECHNICAL DESIGN DESCRIPTION FOR BACK-END OPTICS AND CAMERAS

Sponsored by Oak Ridge National Laboratory
c/o Princeton Plasma Physics Laboratory

Under Subcontract No: S013437

Released 2024/05/28

Released 2024/05/28

Prepared by General Atomics
PO Box 85608
San Diego, CA 92186-5608

GA PROJECT 30424

GENERAL ATOMICS

REVISION HISTORY

Revision	Date	Description of Changes
A	See Watermark	Initial Release

POINT OF CONTACT INFORMATION

PREPARED BY:			
Name	**Position**	**Email**	**Phone**
Colby Conant	Mechanical Engineer	Colby.Conant@ga.com	858-455-3933
APPROVED BY:			
Name	**Position**	**Email**	**Phone**
David Chan	Quality Engineer	David.Chan@ga.com	858-455-3657
Sean McCartney	Lead Engineer	Sean.McCartney@ga.com	858-248-6652
Anthony Gattuso	Program Manager	Anthony.Gattuso@ga.com	858-455-2910

Released 2024/05/28

Released 2024/05/28

TABLE OF CONTENTS

REVISION HISTORY ..... **II**
POINT OF CONTACT INFORMATION ..... **II**
ACRONYMS ..... **VIII**
1 INTRODUCTION **1**
1.1 Purpose 1
1.2 Scope 2
1.3 Definitions 2
1.3.1 Units 2
1.3.2 Coordinate Systems 2
1.3.3 Geometry 2
2 BACK END OPTICS & CAMERAS (BEOC) SUBSYSTEM OVERVIEW **3**
2.1 Key Functions 3
2.2 Primary Subassemblies 3
2.3 Functional Flow Block Diagram 6
2.4 BEOC Subsystem Size, Weight, and Power (SWaP) 7
3 BEOC DETAILED DESIGN SUMMARY **10**
3.1 Optical Layout 10
3.1.1 A70 – Full Spectra Windows and Mirrors 10
3.1.2 A80 – Infrared Mirrors and Field Lens 11
3.1.3 A90 – Infrared Lens Array 11
3.1.4 A100 – Visible Mirrors and Achromatic Doublet 12
3.1.5 A110 – Visible Lens Arrays 13
3.1.6 Visible Filter Wheel Assemblies 14
3.1.7 Calibration Optics and Sources 14
3.2 Opto-Mechanical Design 15
3.2.1 Optical interface - Optic Retention and Flexure Design 15
3.2.2 Optical Mount Assemblies 19
3.3 Visible Filter Wheel Assembly 27
3.3.1 Design Overview 27
3.3.2 Filter Selection Matrix 29
3.3.3 Stepper Motor Operation 29
3.4 Cameras 30
3.4.1 IR Cameras 30
3.4.2 VIS Cameras 30
3.5 Structures and enclosure 31
3.5.1 Optical Bench Assembly 31
3.5.2 Shielded Cabinet Assembly 35
3.6 BEOC Interfaces and Services 41
3.6.1 Interface plate 41
3.6.2 Electrical services 43
3.6.3 Cooling services 45
3.6.4 Beam Shrouds 46
3.6.5 Secondary Channel 47
4 INSTRUMENTATION AND CONTROLS **48**
5 REFERENCES **49**

Released 2024/05/28

Released 2024/05/28

APPENDIX A OPTIC LOAD AND STRESS CALCULATIONS..... A-1
APPENDIX B STEPPER MOTOR OPERATION CALCULATIONS..... B-2
APPENDIX C MATERIAL SUMMARY..... C-1

Released 2024/05/28

Released 2024/05/28

LIST OF FIGURES

Figure 1. Coverage of divertor from a) one UWAVS diagnostic and b) five Upper Port UWAVS diagnostics. 1
Figure 2: 55.GA UWAVS diagnostic system. 3
Figure 3. Back-End Optics and Cameras (doors removed for clarity) 4
Figure 4. BEOC main optical layout 5
Figure 5. BEOC functional flow block diagram 6
Figure 6. BEOC size overview 7
Figure 7. A70 full spectrum optic group. 10
Figure 8. A80 infrared optic group. 11
Figure 9. A90 infrared lens array group with infrared cameras. 12
Figure 10. A100 visible optic group. 13
Figure 11. A110 visible lens array group with visible cameras. 13
Figure 12. Visible filter wheel assemblies mounted to underside of visible bench assembly. 14
Figure 13. Calibration optical layout 15
Figure 14. Detail view of precision and cylindrical pad interfaces on A80-M2 16
Figure 15. Cantilever flexure detail for flat mirrors 16
Figure 16. Detail section view of annular flexure ring on A100-L1L2 17
Figure 17. Threaded retaining ring and spacer application in A90-CH A lens barrel. 18
Figure 18. Detailed interface between threaded retaining rings/spacers and lens 18
Figure 19. Typical pinned interface for BEOC optic mounts on A70-W1 19
Figure 20. Monolithic optic mounts in the UWAVS BEOC. 20
Figure 21. Two-piece kinematic mounts in the UWAVS BEOC. 20
Figure 22. Explode of A100-M2 with Spherolinder kinematic mount detail. 21
Figure 23. Kinematic mount optic cell with mounting tab cone grove detail. 22
Figure 24. Kinematic mirror mount base - v-grove assembly for adjustment 23
Figure 25. Two-piece and monolithic lens cell assemblies. 23
Figure 26. Explode view of A100-L1L2 lens cell assembly. 24
Figure 27. Interface with the polished lens surface negates alignment errors due to (a) tilted rim and (b) decentered rim. 25
Figure 28. Lens array tube assemblies for IR (A90) and VIS (A110) spectrum bands 25
Figure 29. Cross section of A90 IR lens barrel 26
Figure 30. Cross section detail view of A90 lens barrel pilot, threading, and axial shim gap 26
Figure 31. Explode view of visible filter wheel assembly 27
Figure 32. Explode view of populated filter wheel subassembly 28
Figure 33. Visible filter wheel assembly (a) motor interface and (b) position sensor interface. 28
Figure 34. Stepper motor torque vs speed curves for (a) U17-1 and (b) U17-2 magnet sizes 29
Figure 35. Infratec ImageIR 9300 IR Camera with mounted cold plate 30
Figure 36. Visible camera channel A and B mounted on linear stages. 31
Figure 37. BEOC Optical Bench Assembly 32
Figure 38. Main optical bench assembly explode view. 33

Released 2024/05/28

Released 2024/05/28

Figure 39. BEOC Main Optical Bench supporting hardware (a) adjustable bushing, (b) standard pedestal, and (c) pinned pedestal. 33
Figure 40. IR bench assembly....34
Figure 41. Visible optical bench assembly....35
Figure 42. Explode view of shielded cabinet assembly components. 35
Figure 43. Stainless steel gamma shielding structure....36
Figure 44. Port side shifted gamma shielding for clearance and access....37
Figure 45. Neutron shielding B4C brick and assembly into rail channel system. 37
Figure 46. Magnetic iron shielding layer. 38
Figure 47. Detail views of (a) front industrial hinge, (b) bottom caster assembly, and (c) top roller assembly....39
Figure 48. BEOC maintenance door operation (a) first front door swings open, (b) second sliding door, (c) third sliding door, and finally (d) fourth sliding door. 40
Figure 49. BEOC shielded enclosure locking detail views. 41
Figure 50. BEOC interface plate mounted on PCSS with detail view of puck and pedestal hardware. 42
Figure 51. BEOC interface plate alignment pucks facilitate X/Y in plane translation. 42
Figure 52. BEOC enclosure pedestals with (a) pinned interface and (b) standard interface. 43
Figure 53. BEOC electrical service system (1) internal cable routing (2) intermediate adapter cable and (3) PCSS external cable routing. 44
Figure 54. BEOC electrical service disconnects for internal, external and PCSS locations. 45
Figure 55. BEOC cooling services interface at FWD top and internal routing to equipment. 46
Figure 56. BOL to BEOC beam shroud (a) telescoping section and (b) bellow. 46

Released 2024/05/28

Released 2024/05/28

LIST OF TABLES

Table 1. Applicable CAD Models 2
Table 2. BEOC total weight 8
Table 3. BEOC total power consumption 9
Table 4. Visible filter wheel selection matrix 29
Table 5. Material Specification Table C-1

Released 2024/05/28

Released 2024/05/28

ACRONYMS

Acronym	Description
BEOC	Back End Optics & Cameras
BOL	Bio-Shield Optical Labyrinth
CAL	Calibration
CCWS	Component Cooling Water Supply
CG	Center of Gravity
CHWS	Chilled Water Supply
COTS	Commercial Off The Shelf
CTE	Coefficient of Thermal Expansion
EM	Electromagnetic
EWAVS	Equatorial Wide Angle Viewing System
FoS	Factor of Safety
FWD	Forward
IO	ITER Organization
IOT	Interspace Optics Tube
IR	Infrared
IS	Interface Sheet
PC	Port Cell
PCSS	Port Cell Support Structure
PI	Port Integrator
PID	Piping and Instrumentation Diagram
RPS	Rotations Per Second
TGCS	Tokamak Global Coordinate System
UPP	Upper Port Plug
UWAVS	Upper Wide Angle Viewing System
VIS	Visible (light spectrum)

Released 2024/05/28

Released 2024/05/28

1 INTRODUCTION

The 55.GA Upper Port Wide Angle Viewing System (UWAVS) views the divertor in sections and provides machine protection (monitoring for overheating of surfaces), plasma control (basic and advanced), and physics measurement roles. UWAVS is located in UP 2/8 (RFDA), UP 11/14 (USDA) and UP 17 (EUDA). The UWAVS coverage of the divertor is shown in Figure 1.

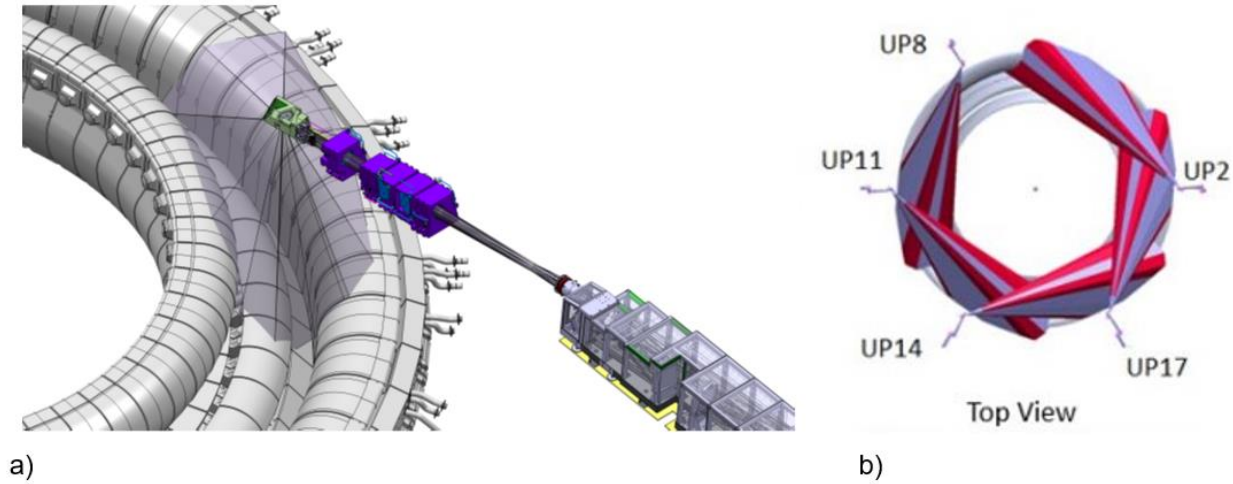

Figure 1. Coverage of divertor from a) one UWAVS diagnostic and b) five Upper Port UWAVS diagnostics.

1.1 Purpose

The purpose of this document is the technical design description (TDD) of the Back End Optics and Cameras (BEOC) subsystem, as part of the ITER diagnostic 55.GA Upper Visible and Infrared Wide Angle Viewing System (UWAVS). The BEOC subsystem resides in the ITER Ex-Vessel Port Cell, and is baselined as a common, identical design between all five installed instances of UWAVS (Upper Ports 2, 8, 11, 14, and 17).

In subsequent sections, the BEOC subsystem design will be described as follows:

- Subsystem overview
- Subsystem and subassembly detailed design summary
- Summary of interfaces and services
- Instrumentation and control scheme summary

Released 2024/05/28

Released 2024/05/28

1.2 Scope

This document provides detailed component design architecture, function, and methodology for the UWAVS (55.GA) BEOC subsystem at the preliminary design phase. The BEOC subsystem design is common for all five Upper Ports (2, 8, 11, 14, and 17).

High-level definitions of the UWAVS system architecture, decomposition, and functions are described in the UWAVS System Design Description Document [1].

1.3 Definitions

1.3.1 Units

The units of the international system (SI) are used unless otherwise stated.

1.3.2 Coordinate Systems

Coordinate system references are consistent with the ITER Tokamak Global Coordinate System [2] unless otherwise stated.

1.3.3 Geometry

The CAD geometry referenced throughout this report is listed below in Table 1.

Table 1. Applicable CAD Models

Model	CAD File
BEOC Assembly	UWAVS_BEOC_SUBSYSTEM_ASSY.CATProduct, A.40

Released 2024/05/28

Released 2024/05/28

2 BACK END OPTICS & CAMERAS (BEOC) SUBSYSTEM OVERVIEW

The UWAVS architecture is based on a modular approach that includes key functional subsystems in and outside of the vacuum vessel as shown in Figure 2. The BEOC serves as the last UWAVS optical subsystem containing conditioning optics and the infrared (IR) and visible cameras.

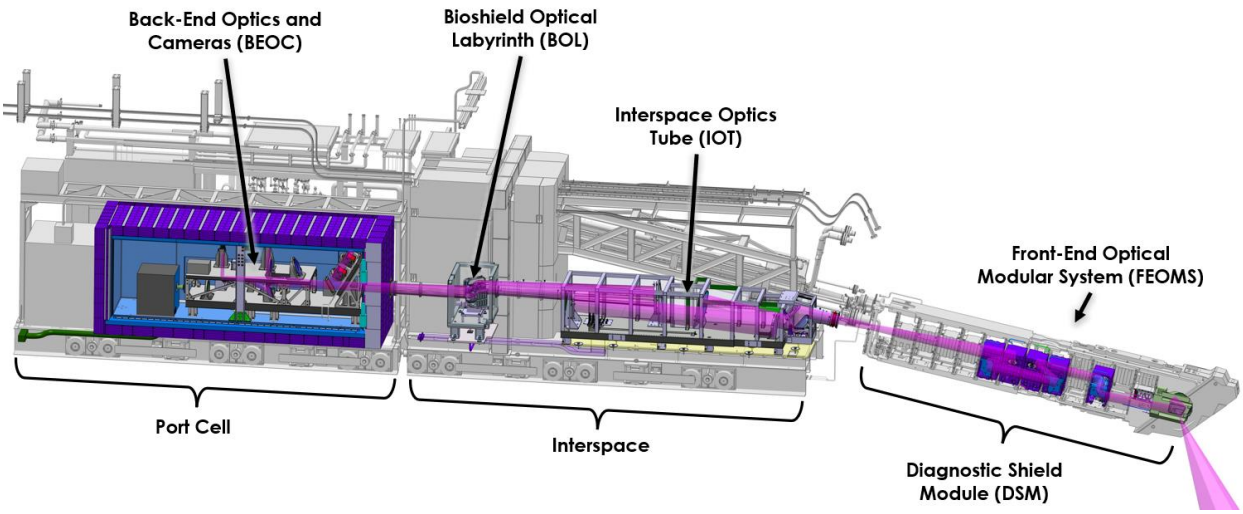

Figure 2: 55.GA UWAVS diagnostic system.

2.1 Key Functions

The BEOC is located behind the Bioshield in the Port Cell (PC), the BEOC mounts to the Port Cell Support Structure (PCSS) via an interface plate and shielded enclosure designed to protect the sensitive electronics and optics from radiation and contamination ingress.

Light enters the BEOC through a shielded shroud from the Bio-Shield Optical Labyrinth (BOL) and passes through a series of windows and mirrors that split the full spectral range into two wavelength bands (Visible and IR). Both IR and visible legs of the optical system consist of two cameras, and have lens doublets and respective fold mirrors and energy splitters to separate the light into two required camera channels. Finally, the wavelength bands are focused onto camera detectors via IR and visible lens arrays.

2.2 Primary Subassemblies

As seen in Figure 3, the BEOC consists of the optical relay system, the optical bench assembly, and the shielded enclosure. The optical bench assembly supports the optical relay system while the shielded enclosure protects the optics and sensitive electronics from both radiation and contamination. The BEOC is mated to the PCSS via an interface plate which allows in-plane translation to adjust for large initial installation tolerances within the Port Cell.

Released 2024/05/28
Released 2024/05/28

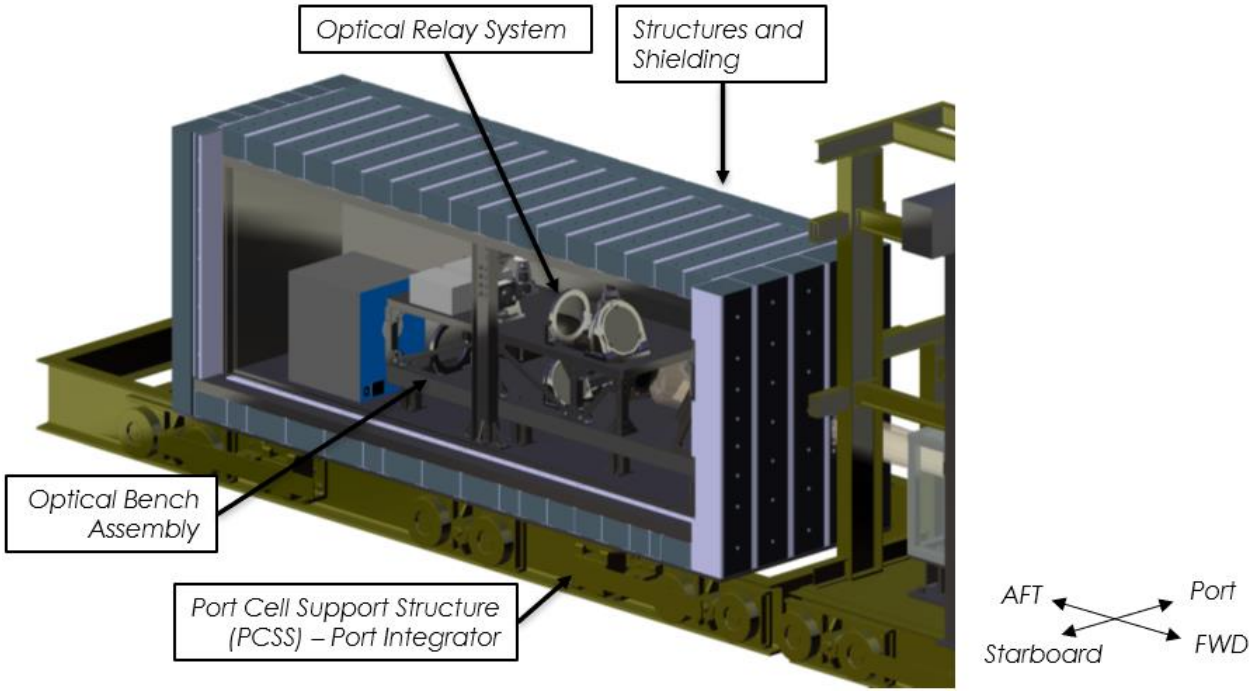

Figure 3. Back-End Optics and Cameras (doors removed for clarity)

The optical relay system shown in Figure 4 is comprised of the A70, A80, A90, A100, A110 optics groups, a pair of filter wheel assemblies, the IR and visible cameras, and the calibration system. The A70 optics group is a set of large windows, beam splitters, and folding mirrors that condition and separate the IR and visible light beams. The A80 optics group consists of a field lens, beam splitter and folding mirrors to direct the two IR frequency band beams to their appropriate cameras. The A90 optics consist of two identical lens tubes to focus an image for the two IR cameras. The A100 optics group consists of an achromatic doublet to correct the color aberration, a beam splitter, and folding mirrors to direct the visible light beams to the two visible cameras. The A110 optics are a set of two lens tubes containing different optics that form an image for the Channel A and Channel B visible cameras.

Released 2024/05/28

Released 2024/05/28

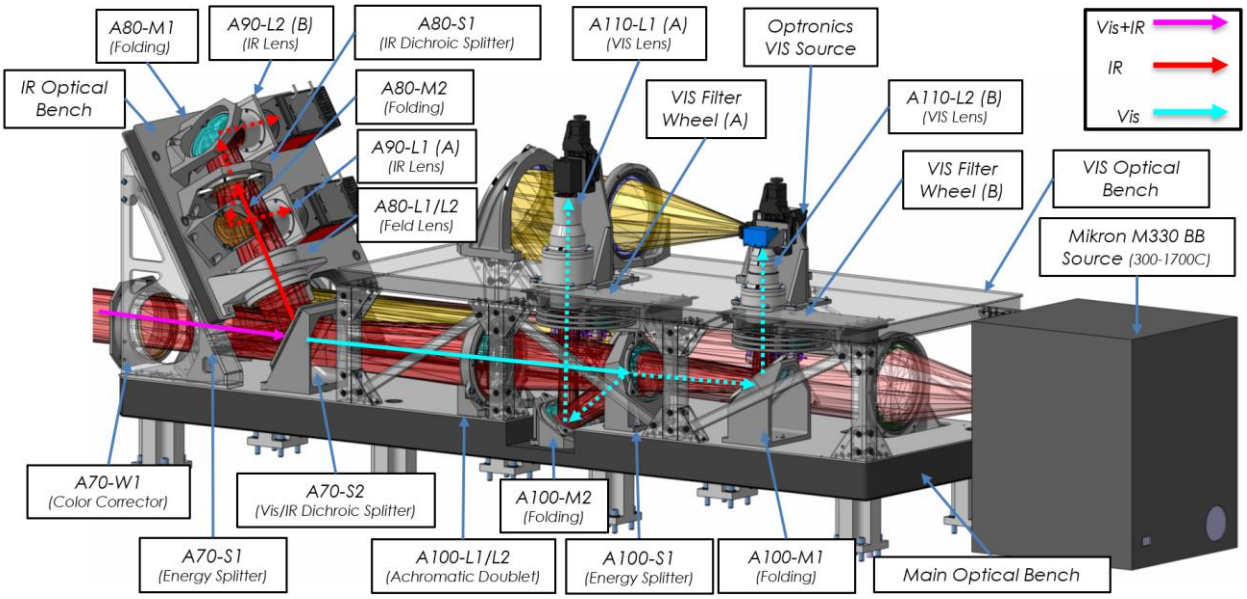

Figure 4. BEOC main optical layout

To ensure accurate IR and visible measurements, a calibration assembly is also nested in the shielded enclosure. The calibration system consists of a set of lens and fold mirrors that bring light from a black body (IR) or integrating sphere (visible) into the into the beam path via the A70-S1 splitter.

Prior to the lens tubes, a modular, actuated filter wheel assembly will be placed containing filters to isolate 10 frequency bands for the observation of specific elements as well as a set of neutral density filters. These filter wheel assembly modules are accessible for replacement in the event of a failure or desire for alternate filters.

The BEOC is exposed to lesser radiation and elevated temperature than the IOT and BOL, but not an inconsequential amount. In this case, the BEOC is enclosed in layers of shielding to minimize radiation and electromagnetic (EM) exposure, protecting electronics and cameras inside.

Released 2024/05/28

Released 2024/05/28

2.3 Functional Flow Block Diagram

Figure 5 shows the BEOC subsystem block diagram that highlights function, decomposition, and key mechanical, optical, electrical, and cooling interfaces. Color codes and line types are noted in the legend.

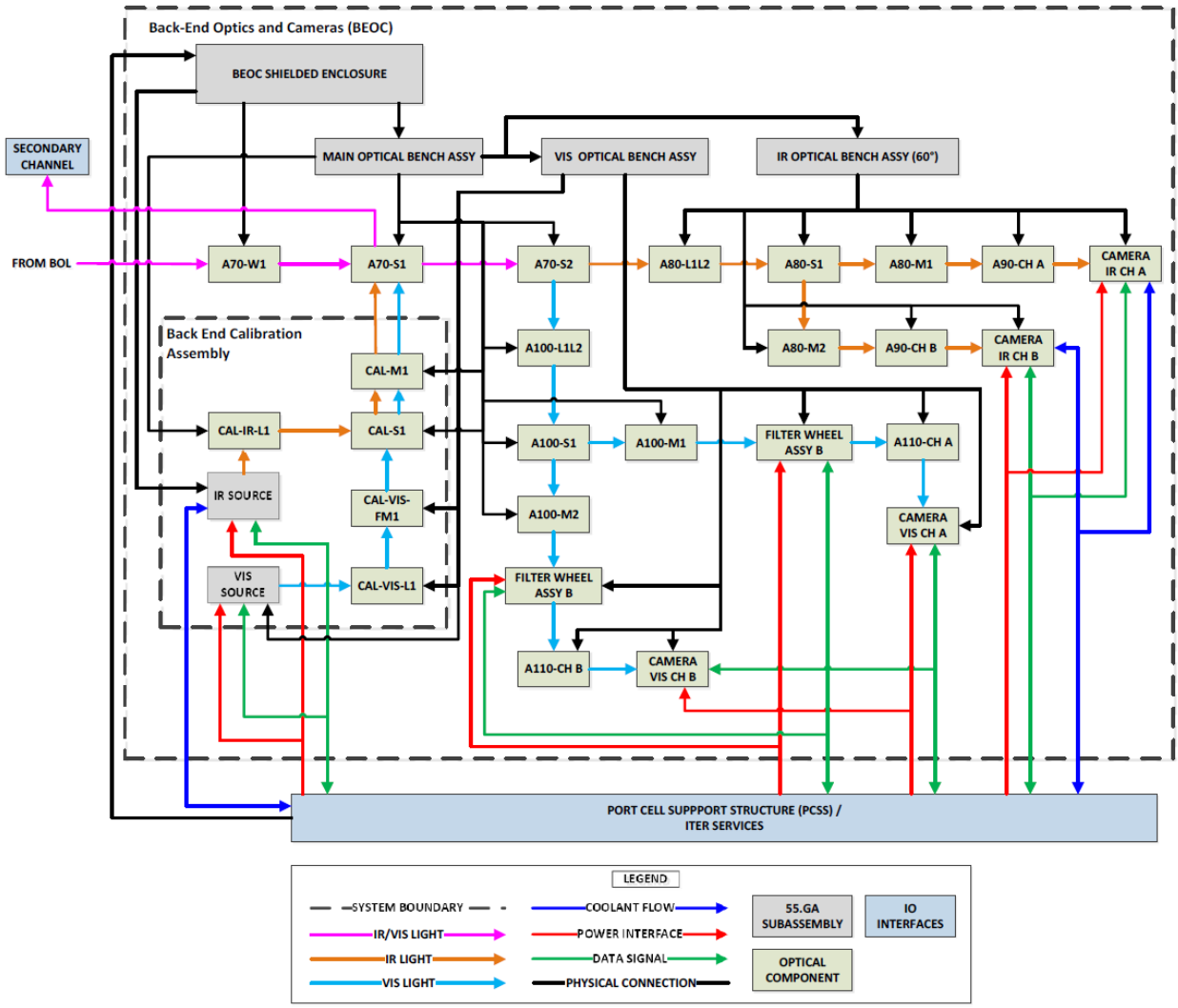

Figure 5. BEOC functional flow block diagram

Released 2024/05/28

Released 2024/05/28

2.4 BEOC Subsystem Size, Weight, and Power (SWaP)

The BEOC SWaP is closely tracked to ensure requirements are met as well as provide inputs for subsequent structural, thermal, and optical analysis. The size and volume of the BEOC in Figure 6 fits within the allocated space claim. BEOC weight and power is shown in Table 2 and Table 3 respectively. A list of high-level component materials can be found in APPENDIX C .

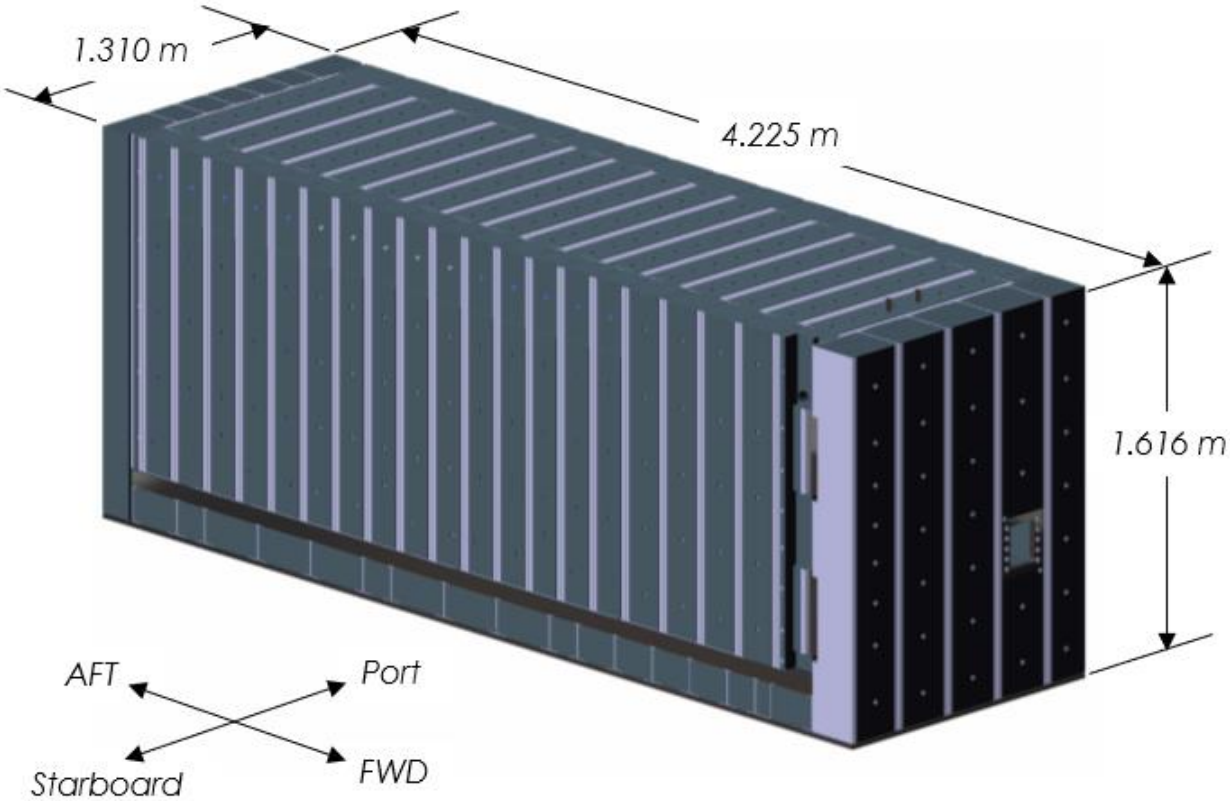

Figure 6. BEOC size overview

Released 2024/05/28

Released 2024/05/28

Table 2. BEOC total weight

						Total Weight (kg)	Total Volume (m^3)
						22935.71	8.94
Item	Part Number	Component	Qty	Weight (kg)	Volume (m^3)	Total Weight (kg)	Total Volume (m^3)
Optical Bench Assy						467.51	
		Main optical bench assy					
		Main optical bench	1	191.14	0.01	191.14	
		Main bench post	4	12.00		48.00	
		Main bench post - pinned	2	12.00		24.00	
		IR Breadboard assy					
		IR breadboard	1	34.06	0.01	34.06	
		IR Bench Support	1	26.45		26.45	
		VIS Breadboard assy					
		VIS Breadboard	1	103.61		103.61	
		VIS Bench Support	1	40.25		40.25	
Optical Relay System - Main Path						99.57	
		A70-W1	1	3.73		3.73	
		A70-S1	1	2.57		2.57	
		A70-S2	1	5.95		5.95	
		A80-L1L2	1	10.57		10.57	
		A80-S1	1	3.32		3.32	
		A80-M1	1	2.77		2.77	
		A80-M2 (D-shape)	1	1.91		1.91	
		A90-Channel A	1	8.42		8.42	
		A90-Channel B	1	8.42		8.42	
		A100-L1L2	1	7.22		7.22	
		A100-S1	1	3.29		3.29	
		A100-M1	1	4.44		4.44	
		A100-M2	1	2.96		2.96	
		A110-Channel A	1	9.10		9.10	
		A110-Channel B	1	5.48		5.48	
		Filter Wheel Assy	2	9.712		19.42	
Optical Relay System - Calibration Optic						39.32	
		CAL-VIS-L1	1	5.834		5.83	
		CAL-VIS-FM1	1	8.407		8.41	
		CAL-IR-L1	1	4.893		4.89	
		CAL-S1	1	3.284		3.28	
		CAL-M1	1	6.071		6.07	
		Heat shielding	1	10.832		10.83	
Cameras / Electronics						105.21	
	Infratec 9300	IR Camera	2	4		8.00	
	Emergent HT-12000	VIS Camera 1	1	0.34		0.34	
	Mikrotron EoSense 4CXP	VIS Camera 2	1	0.45		0.45	
	Mikron M330	IR blackbody source	1	80		80.00	
	Optronic OL 458-4	VIS integrating sphere	1	2.618		2.62	
	Comet AGS 4010a 7-16	RF Matching Box	2	6.9		13.80	
Structures and Shielding						22224.10	
		Shielding Assembly	1	21424.80		21424.80	
		PCSS Interface plate + hdwr	1	799.3		799.30	

Released 2024/05/28

Released 2024/05/28

Table 3. BEOC total power consumption

Item	Part Number	Description	Qty	Power Dissipation (W)	Total Power (W)	Op Temp. Non-op Temp. (C)	Relative Humidity (%, Non Condensing)
1	Infratec Image IR 9300	IR Camera	2	27	54	Op: -20 to 50 Non-Op: -40 to 70	-
2	EMV HT-12000	VIS Camera 1	1	9	9	Op: 0 to 45 Non-Op: -30 to 60	-
3	Mikrotron Eosens 4CPX6	VIS Camera 2	1	10	10	Op: -20 to 40 Non-Op: -40 to 80	0 to 93
4	Mikron M330	IR black body source	1	3000	3000	Op: 0 to 44 Non-Op: -20 to 80	0 to 90
5	Optronic OL 458-4	VIS integrating sphere	1	4.8	4.8	Op: 0 to 35 Non-Op: -	0 to 90

Released 2024/05/28

Released 2024/05/28

3 BEOC DETAILED DESIGN SUMMARY

3.1 Optical Layout

In the following sections, the optics are decomposed by form and support function to highlight beam conditioning roles of each optic.

3.1.1 A70 – Full Spectra Windows and Mirrors

The A70 group in Figure 7 is the first set of optics in the relay system and is comprised of the A70-W1 sapphire corrector, A70-S1 energy splitter, and A70-S2 dichroic splitter. The A70-W1 assembly is a 200x10mm sapphire optic housed in a monolithic, 6061-T6 aluminum mount, fixed to the forward BEOC shielded wall. A70-W1 optic is positioned at an angle which corrects for slight color aberrations caused by the downstream vacuum window. The dual function A70-S1 houses a thinner, 1mm thick sapphire optic in a monolithic 6061-T6 aluminum mount fixed to the main optical bench assembly. The first function of the A70-S1 optic is to direct roughly 10% of the full spectra light to the optional secondary channel and the second function is to direct light from the calibration optical leg into the main beam path. The last assembly, A70-S2, splits the broad spectrum light into visible and IR bands. Due to the need for alignment of the dichroic splitter, the A70-S2 assembly is comprised of a two piece 6061-T6 aluminum mount that allows adjustment between the base and optic cell. The A70-S2 optic is a 200x145mm fused silica substrate at a 2.2 degree wedge.

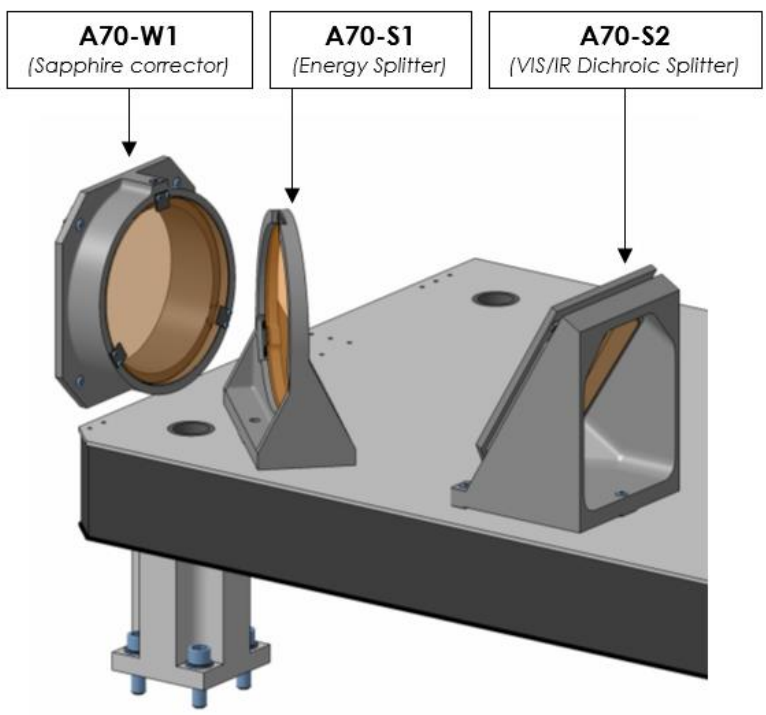

Figure 7. A70 full spectrum optic group.

Released 2024/05/28

Released 2024/05/28

3.1.2 A80 – Infrared Mirrors and Field Lens

The A80 optics group in Figure 8 is the first of two groups in the IR leg and resides on the IR optical bench at a 60 degree angle with respect to the main optical bench. Once IR light is directed upward by the A70-S2 dichroic it passes through the A80-L1L2 field lens assembly. Two lenses within A80-L1L2 assembly are retained in a 304 stainless steel lens barrel via 180mm diameter retaining rings. The A80-L1L2 lens assembly reduces pupil aberrations at the cold stop in the IR cameras, increasing signal to noise ratio for better imaging. Following the field lens assembly are two similar two piece 6061-T6 aluminum mount assemblies, A80-S1 and A80-M1 which allow for IR wavelength separation and beam steering into the Channel B lens and camera respectively. Due to tight space constraints and proximity to the beam, the A80-M2 mirror assembly is a 6061-T6 aluminum monolithic mount which houses a D-shaped 118mm diameter optic which directs light into the Channel A lens and camera.

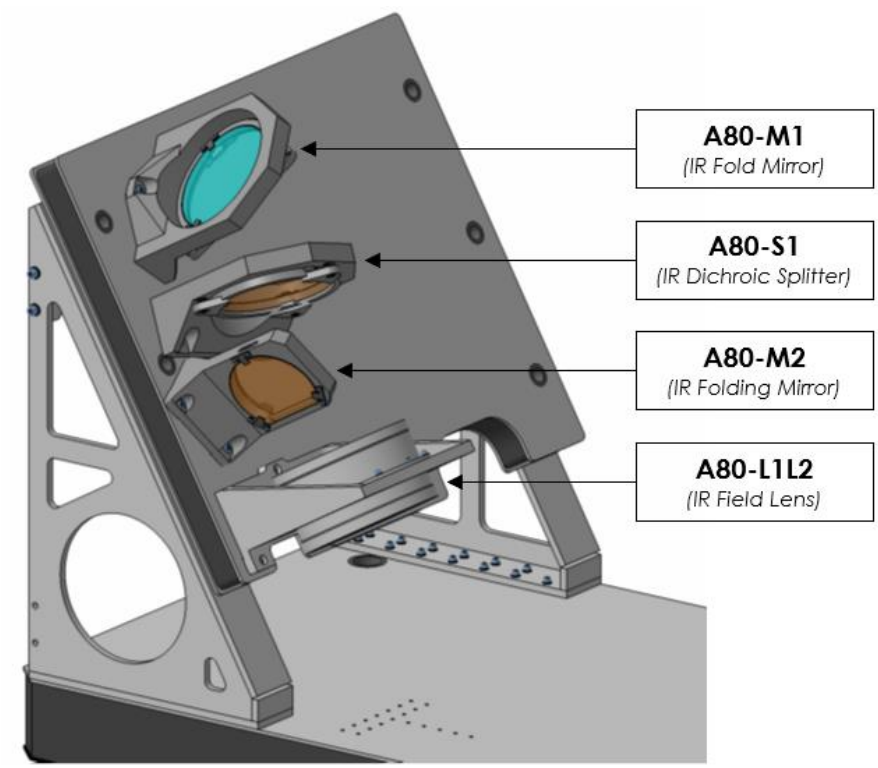

Figure 8. A80 infrared optic group.

3.1.3 A90 – Infrared Lens Array

The A90 optics group in Figure 9 is the last group in the IR leg and consist of two identical lens tubes to focus an image for the two IR cameras. The two piece lens barrels are held horizontally by a 304SS base about the center of gravity (CG) and retain seven lenses of varying sizes and substrates. The two-piece lens barrel eases assembly and provides an interface to adjust for axial focus compensation.

Released 2024/05/28
Released 2024/05/28

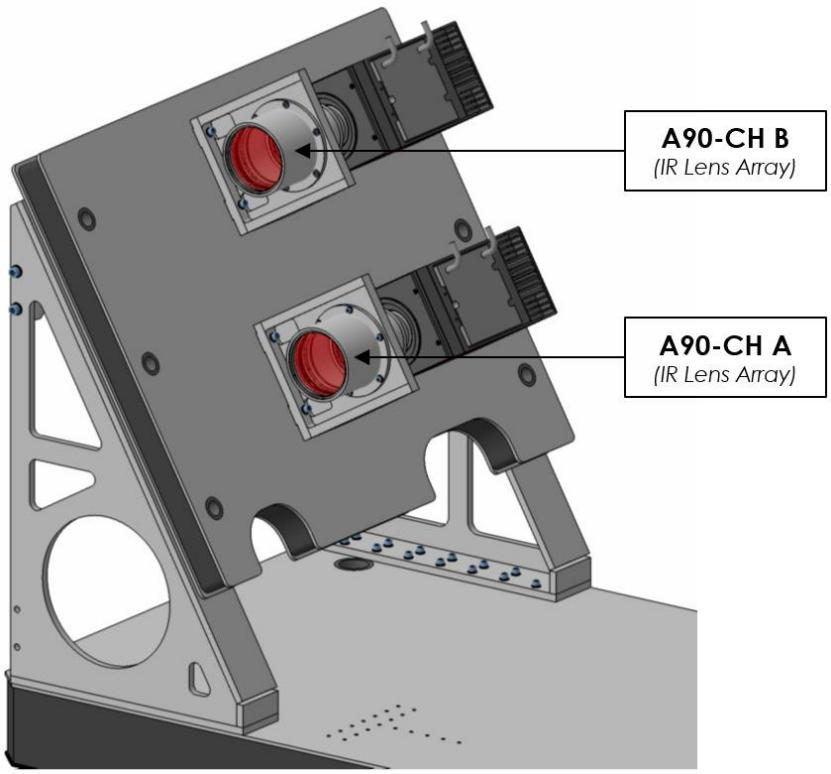

Figure 9. A90 infrared lens array group with infrared cameras.

3.1.4 A100 – Visible Mirrors and Achromatic Doublet

The A100 optics group in Figure 10 is the first of two groups in the visible leg and resides on the main optical bench. Visible light transmits through A70-S2 and interfaces with A100-L1L2 achromatic doublet assembly. The A100-L1L2 lenses correct for spherical and chromatic aberrations and act as the first lens in the imaging telescope for the visible channel. The 230mm diameter achromatic doublet lenses are retained in a 6061-T6 aluminum lens cell and base with 17-7 stainless steel annular flexures. Following the A100-L1L2 assembly the visible light is split by A100-S1 50/50 energy splitter and directed to the visible lens tubes by A100-M1 and A100-M2. A100-S1, A100-M1, and A100-M2 are all similar two-piece kinematic designs, differing only by their base which holds the mirror cells at their required angle and height. The two-piece kinematic optic mount design facilitates beam steering and alignment into the visible lens tubes and cameras.

Released 2024/05/28

Released 2024/05/28

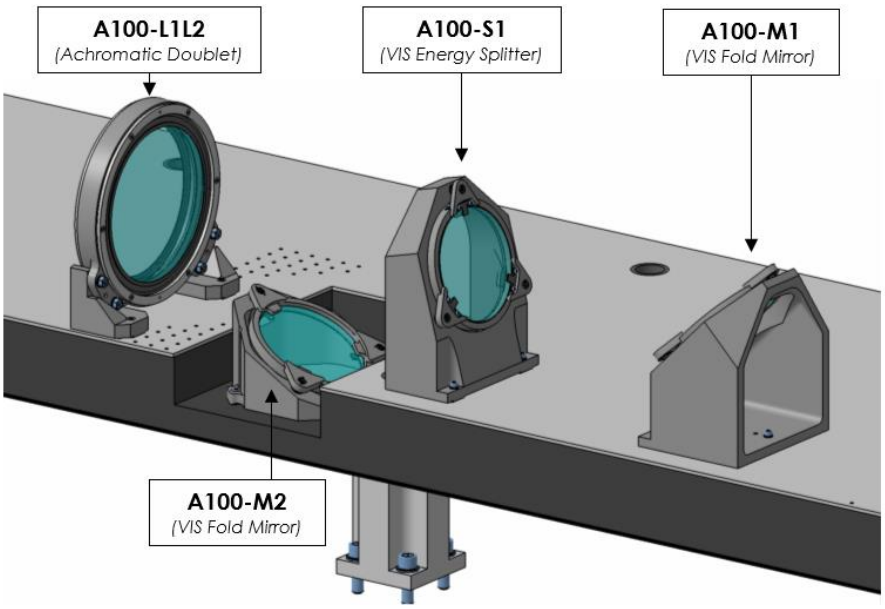

Figure 10. A100 visible optic group.

3.1.5 A110 – Visible Lens Arrays

The A110 optics group in Figure 11 is the last group in the visible leg and consist of two different lens tubes to focus an image for the two VIS cameras. The two-piece lens barrels are held vertically by a 304SS base about the center of gravity (CG) and retain nine lenses of varying sizes and substrates. The two-piece lens barrel eases assembly and provides an interface to adjust for axial focus compensation. Camera model and sensor sizes differ between Channel A and B, therefore two lens barrel designs were required to create the correct image size.

Released 2024/05/28

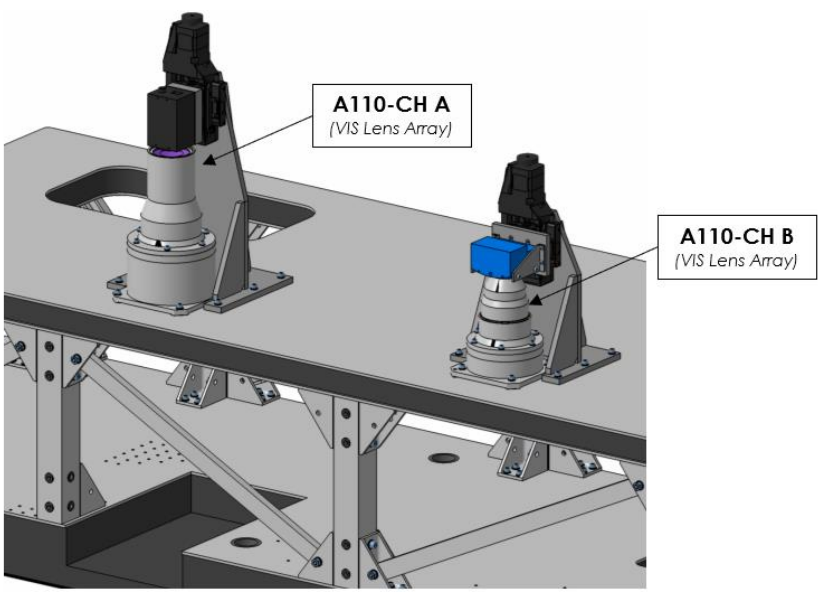

Released 2024/05/28

Figure 11. A110 visible lens array group with visible cameras.

3.1.6 Visible Filter Wheel Assemblies

Prior to the visible lens tubes, a modular, actuated filter wheel assembly is mounted containing filters to isolate 10 frequency bands for the observation of specific elements as well as a set of neutral density filters. Three external gear tooth filter wheels stack in a housing enclosure and are actuated by radiation hardened stepper motors. Filter wheel position is sensed by a radiation hardened mechanical sensor that interfaces with a cam lobe on each wheel. The two visible filter wheel assemblies are mounted to the underside of the visible optical bench assembly via M6 screws as seen in Figure 12.

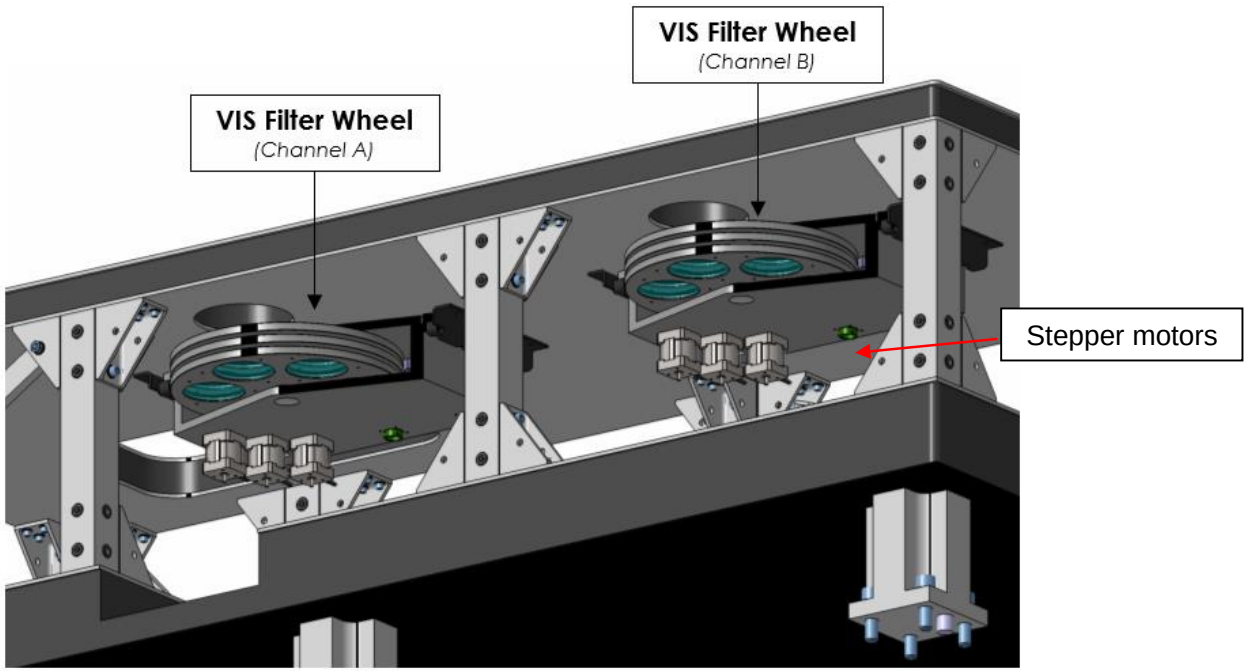

Figure 12. Visible filter wheel assemblies mounted to underside of visible bench assembly.

3.1.7 Calibration Optics and Sources

The calibration system consists of a set of lens and fold mirrors that bring light from a black body source (IR) or integrating sphere (visible) into the beam path via the A70 splitter. The two-level optical layout shown in Figure 13 has the visible leg mounted on the visible optical bench assembly and the IR leg mounted to the main optical bench assembly. Visible light is directed down to the main optical bench by CAL-VIS-FM1 and is combined with the IR leg via CAL-S1 dichroic splitter. The opto-mechanical construction of the calibration mounts uses the same design methods as the main optical path mounts.

Released 2024/05/28

Released 2024/05/28

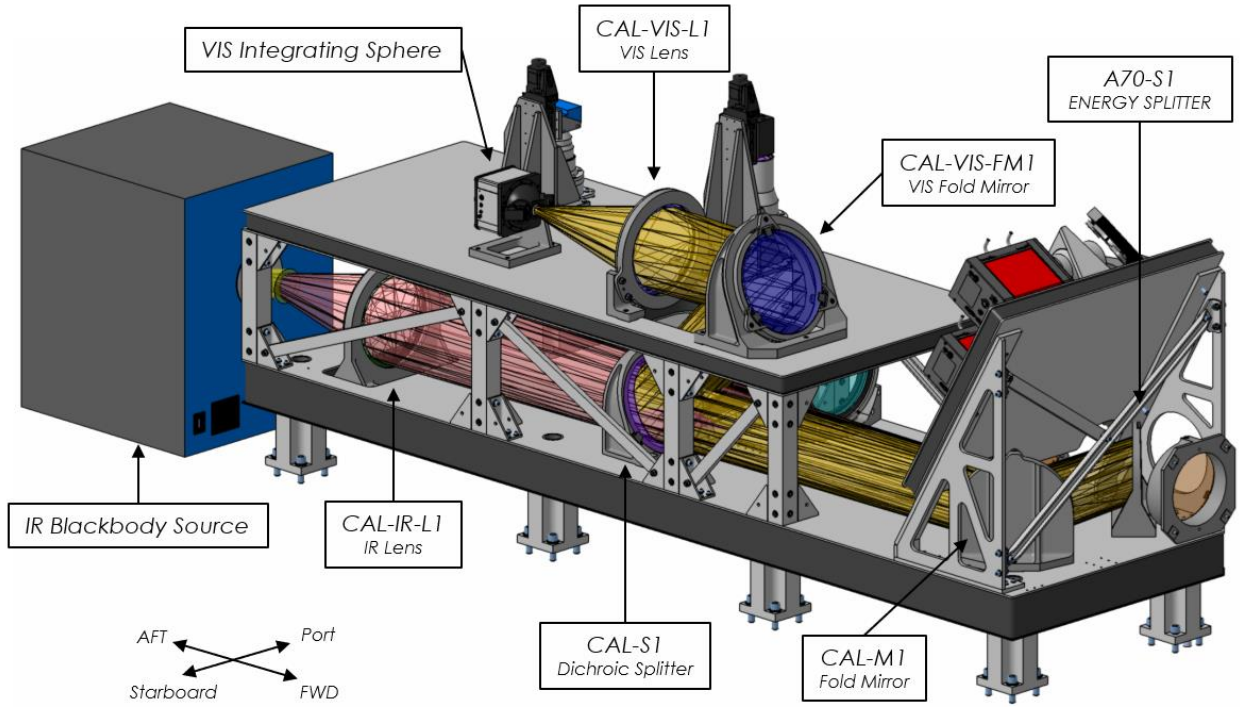

Figure 13. Calibration optical layout

3.2 Opto-Mechanical Design

3.2.1 Optical interface - Optic Retention and Flexure Design

3.2.1.1 Retaining and Mounting Stresses

For nonmetallic mirrors (optical crystals) and lenses, flexures or threaded retaining rings are implemented to adequately secure the optic to its respective metallic mount. Retention forces are designed to keep the optic secure and within stress limits during exposure to a 5g acceleration.

Unlike metals with well-established mechanical properties and damage thresholds, failure parameters for glass can vary greatly. Since brittle glass and ceramics typically fail in tension versus compression, tensile stresses are used as the design criteria for optic retention. A widely accepted threshold of 6.9 MPa (1 ksi) in [3] has proven to be 2-3 times greater on precision manufactured optical components [4]. In lieu of testing optic substrate samples for properties, a more relevant industry standard tensile stress tolerance of 13.8 MPa (2 ksi) is used as a threshold for calculation and analysis in APPENDIX A .

3.2.1.2 Cantilever flexures

For flat mirrors and splitters, the optic face is set on three precision pads held to tight tolerances directly opposing the flexures. The optic edge is registered on two cylindrical pads, creating a line contact about the thickness. Details for both precision and cylindrical pads are highlighted in

Released 2024/05/28
Released 2024/05/28

Figure 14. This semi-kinematic approach eliminates bending stress from the flexure force and reduces the possibility of over constraining contacts. To constrain all degrees of freedom, three flexures provide force to register the optic against its face while one or more flexures register the optic about its edge. Rotation about optical axis Z is constrained by friction forces against the optical surface, face flexures, and opposing metallic surfaces.

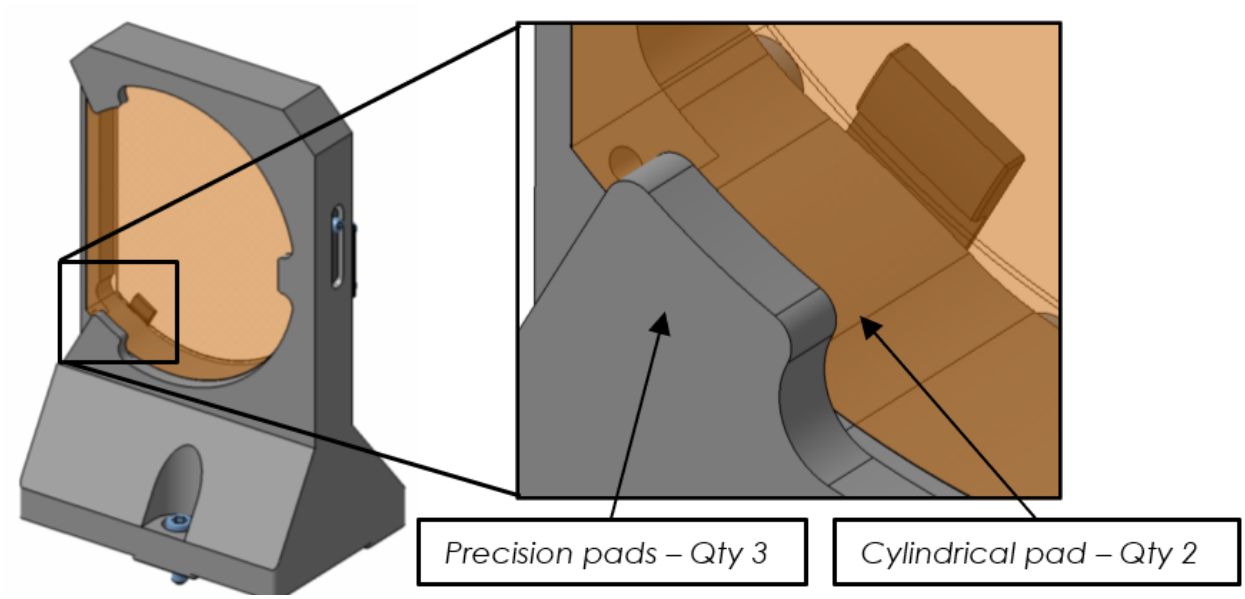

Figure 14. Detail view of precision and cylindrical pad interfaces on A80-M2

Cantilever flexures are designed as 17-7 stainless steel beams fixed at one end, typically by one or two screws, that contact the optic at the opposing end with a cylindrical surface. To provide the required spring force, the flexures are deformed at the optic interface to a predetermined displacement. This displacement can be fine-tuned via shims as shown in Figure 15.

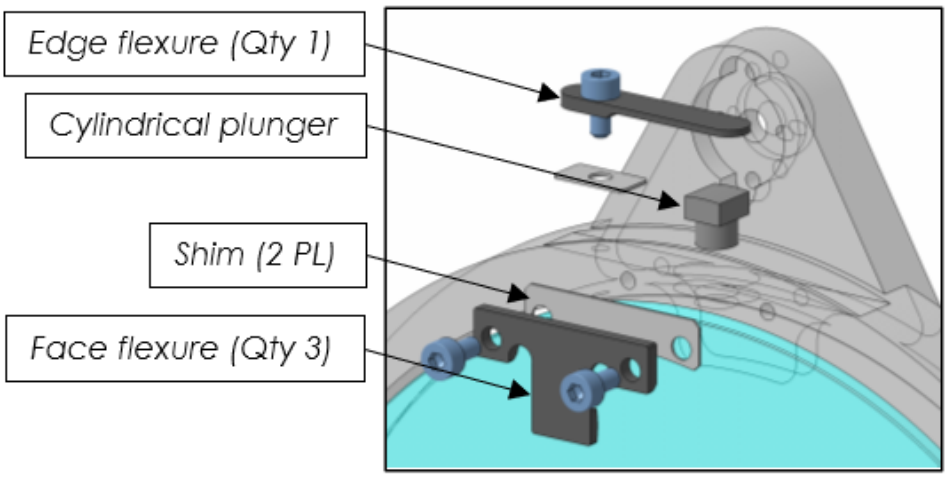

Figure 15. Cantilever flexure detail for flat mirrors

Released 2024/05/28

Released 2024/05/28

3.2.1.3 Annular flexures

Large diameter, heavier lenses in the system leverage large 17-7 stainless steel annular flexures. The annular flexure design principles are consistent with cantilever flexures where the outer perimeter of the disc is restrained to the cell by a bolted flange and the inner perimeter interfaces with the curved optic surface. To reduce stress concentrations at the optic interface when deflected, a large radius is machined into the 17-7 stainless steel flexure at the inner circumference. Figure 16 shows a detailed section view of A100-L1L2 annular flexure, retaining flange, and line of force for the two achromatic doublet lenses.

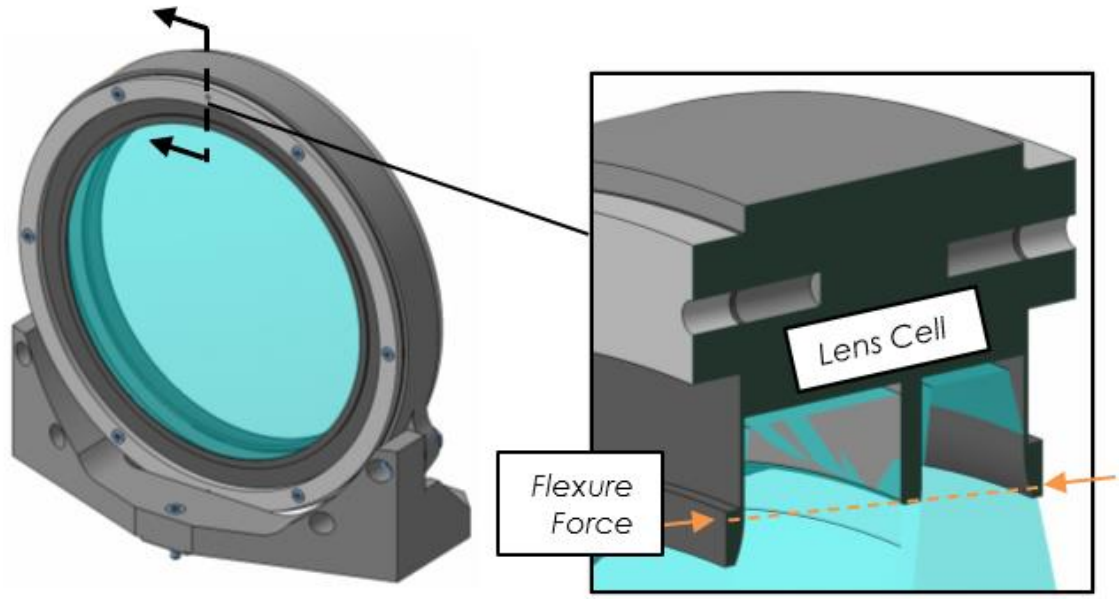

Figure 16. Detail section view of annular flexure ring on A100-L1L2

3.2.1.4 Threaded retaining rings

For smaller diameter lenses, 304 stainless steel threaded retainer rings and spacer rings position and secure the optics within the lens barrels. Spacers can be precisely machined to tight tolerances to accurately locate the lenses, ensuring proper alignment. Retaining rings can be torqued to a desired preload and then staked in place with low-outgassing epoxy. Where possible, COTS sized retaining rings are used within the lens barrels however for larger lenses custom rings are required. A typical application of a lens positioned with a spacer and secured with a threaded retaining ring is depicted in Figure 17.

Released 2024/05/28

Released 2024/05/28

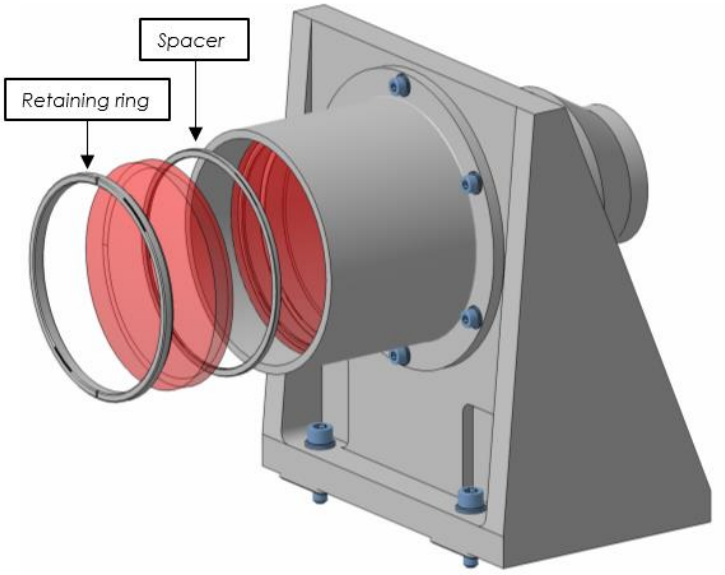

Figure 17. Threaded retaining ring and spacer application in A90-CH A lens barrel.

In an effort to improve alignment accuracy while simultaneously mitigating stress concentrations, threaded retainers and spacers have a sharp edge contact at an obtuse 135 degree angle (Figure 18). Sharp corner interfaces provide the highest accuracy of axial position, however they have the potential for large contact stresses. An obtuse angle versus a typical 90 degree angle reduces the chance of stress concentrations by eliminating burs left from machining while maintaining the exact location of the optical interface needed for accurate lens positioning.

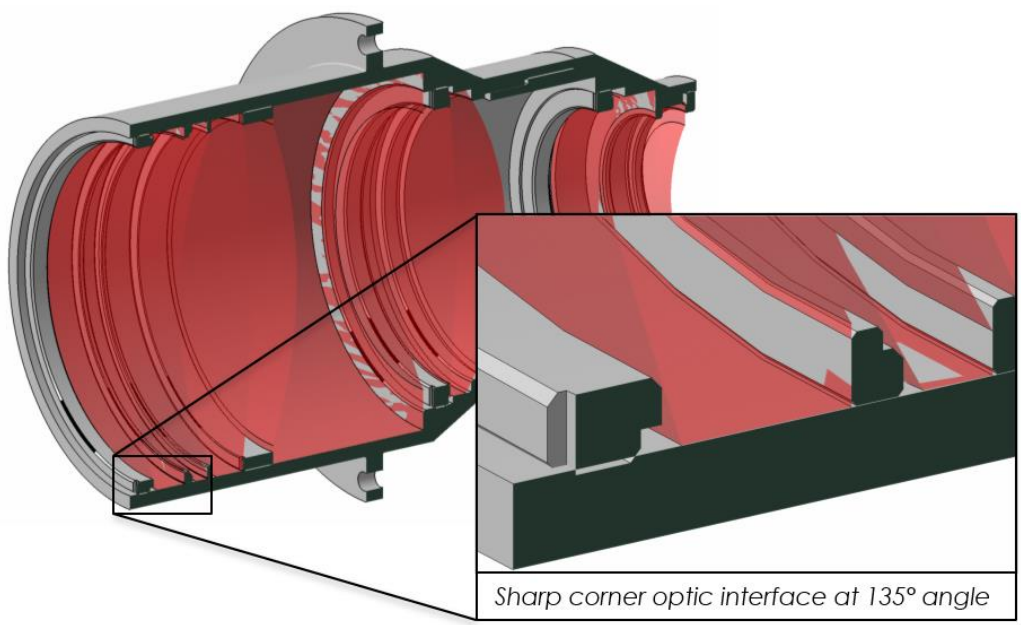

Figure 18. Detailed interface between threaded retaining rings/spacers and lens

Released 2024/05/28

Released 2024/05/28

3.2.2 Optical Mount Assemblies

The optical elements located in the BEOC vary in size and orientation, requiring unique optical mounts to properly fix to their respective bench or structure. Although each optic requires a unique mount, common design methods are used across all assemblies. Common optic mount groups can be broken out into four subsequent categories.

Each mount is pinned to its respective interface for alignment and bolted via M6 hardware. Raised pads located at each bolted interface are held to tight profile tolerances ensuring coplanarity while also alleviating flatness requirements for the entire base. Figure 19 shows a typical pinned interface with raised mounting pads on A70-W1. When possible, interface pads are limited to three to alleviate over-constraining the optic mount.

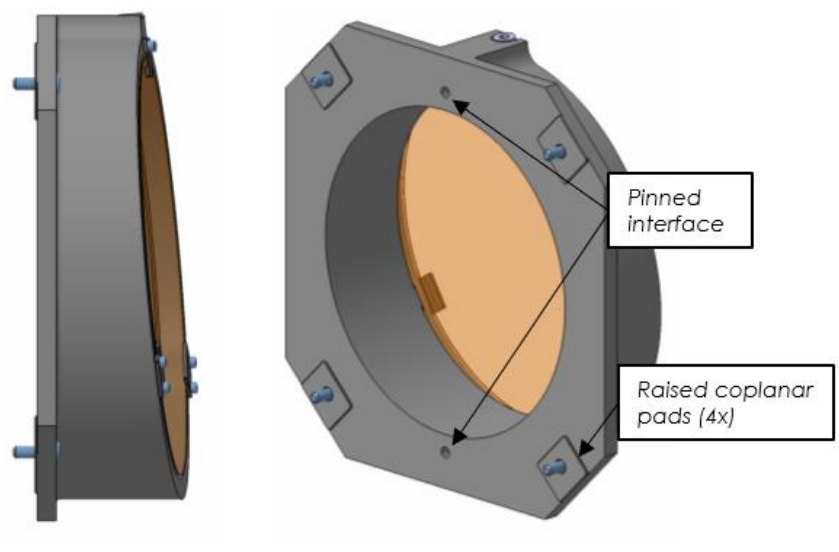

Figure 19. Typical pinned interface for BEOC optic mounts on A70-W1

3.2.2.1 Monolithic optic mount assemblies

Monolithic optic mounts in Figure 20 are designed for optics located in tight spaces or in instances where optical adjustment is not required.

Released 2024/05/28

Released 2024/05/28

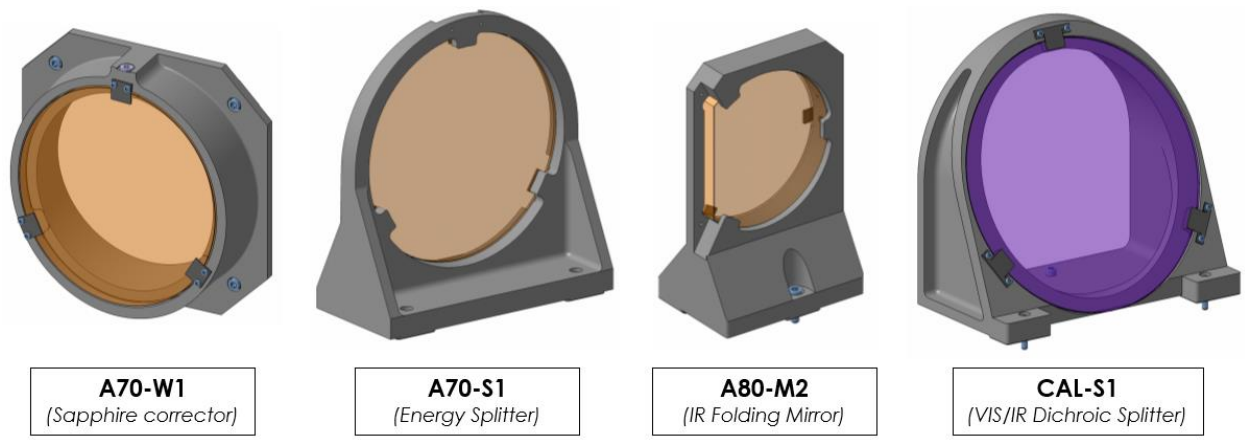

Figure 20. Monolithic optic mounts in the UWAVS BEOC.

As the description indicates, monolithic mounts are single piece, machined mounts made of 6061-T6 aluminum. Aluminum is used over stainless steel for optic mounts and cells to reduce weight and stress at the optic interface. In comparison to stainless steel, aluminum has a lower elastic modulus and higher Poisson ratio allowing more elastic deformation at the optic interface, therefore increasing the contact surface and reducing stress. Cantilever flexures retain the optics as described in Section 3.2.1.2.

3.2.2.2 Kinematic optic mount assemblies

Two-piece kinematic optic mounts in Figure 21 are designed for instances where optical alignment compensation is needed.

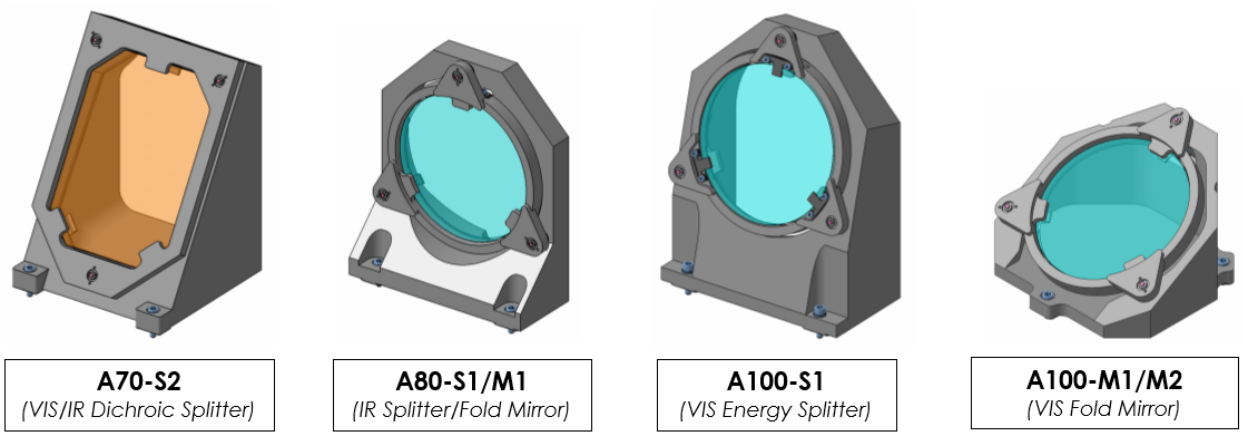

Figure 21. Two-piece kinematic mounts in the UWAVS BEOC.

Released 2024/05/28

Released 2024/05/28

The two main components of the mount being the optic cell and base are joined via a COTS kinematic Spherolinder mechanism from G2 Engineering [5]. The Spherolinder mechanism depicted in Figure 22 is comprised of a captive fastener with four components: 1) V-groove, 2) cone grove, 3) center Spherolinder, and 4) fastener stud which are all 400 series stainless steel. To tip, tilt, and translate the optic cell with respect to the base, shims are placed between the Spherolinder V-groove and base mounting surface shown in Figure 22.

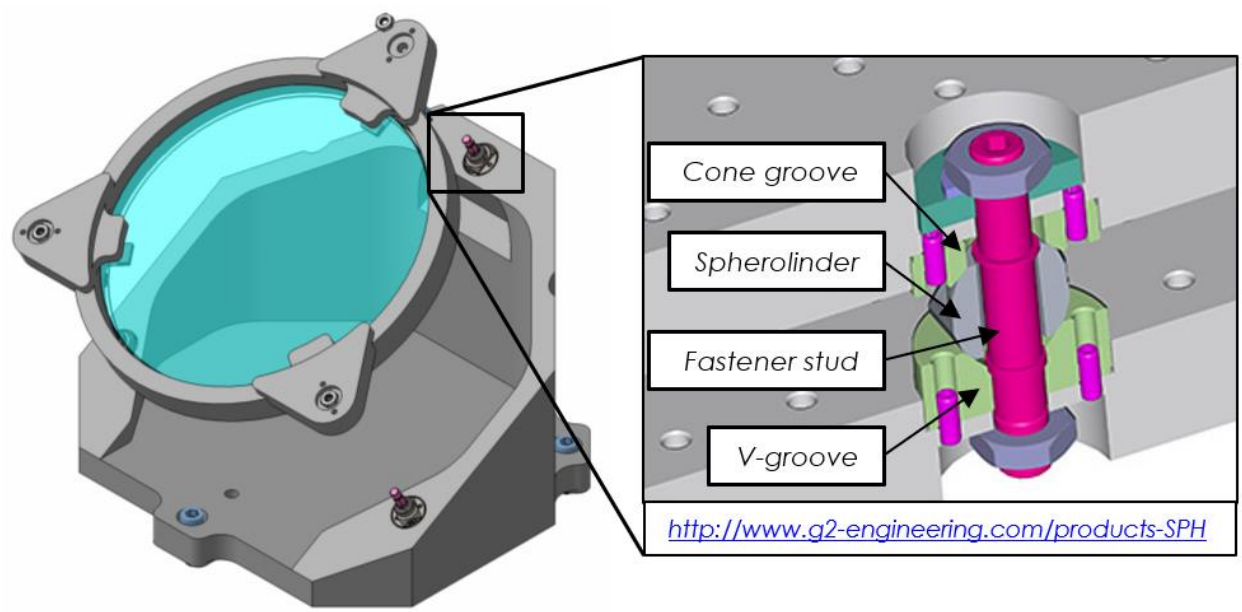

Figure 22. Explode of A100-M2 with Spherolinder kinematic mount detail.

The optic resides in the optic cell and is restrained via cantilever flexures described in Section 3.2.1.2. The cell is made of 6061-T6 aluminum and is mated to the base at three points on tabs around the perimeter of the optic by the kinematic Spherolinder fasteners. On the underside of the mounting tab in Figure 23, the cone groove portion of the Spherolinder is located by 2mm pins and fastened via two M3 screws. Efforts were made to create common cells for optics of similar form and size.

Released 2024/05/28

Released 2024/05/28

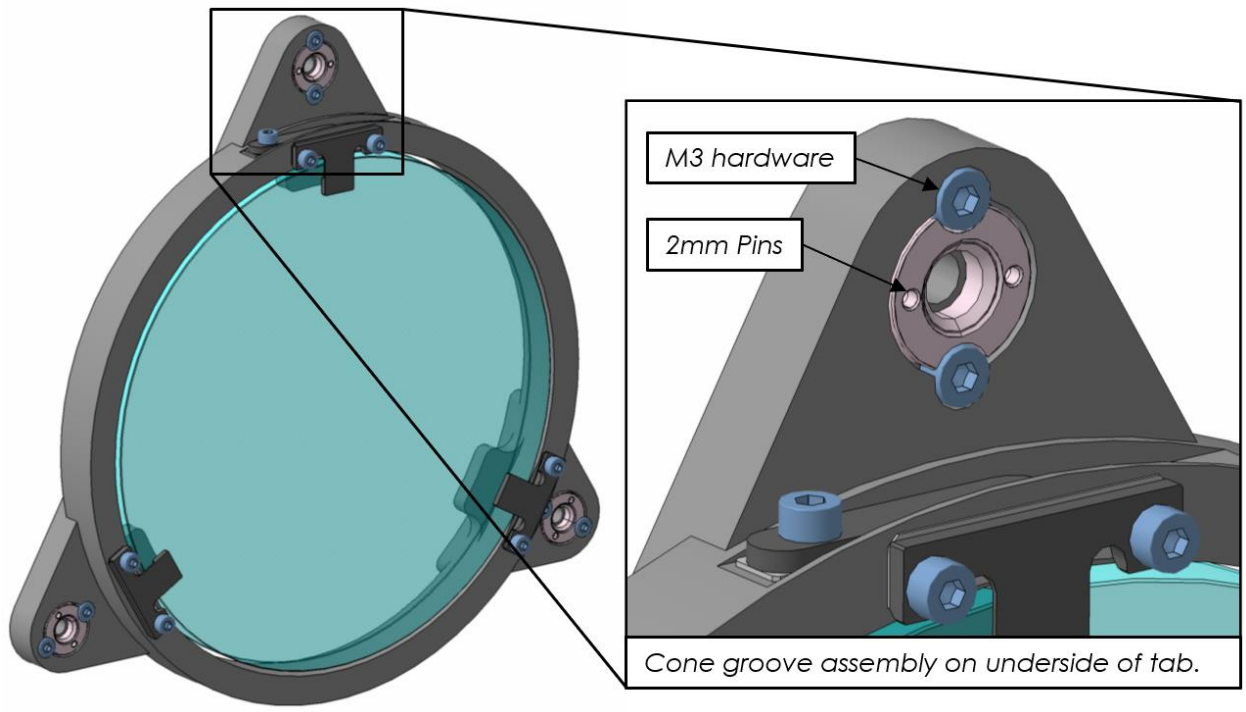

Figure 23. Kinematic mount optic cell with mounting tab cone grove detail.

The 6061-T6 aluminum base bridges the gap between the optic cell and respective mating optical bench or structure. Bases are unique to each optic within the BEOC due to varying angles, positions, and proximity to structures. The Spherolinder V-groove components are positioned in a kinematic “triple vee” orientation so that all grooves point toward the center of the mounting patter at the centroid of the optic (Figure 24). The benefit of the “triple vee” over other kinematic orientations (i.e., cone/vee/flat), is the optic cell self-centers about the centroid of the mounting points. Therefore, when the mount is subject to temperature variations and components shift due to material coefficients of thermal expansion (CTE), the center of the optic remains in position at the centroid.

Released 2024/05/28

Released 2024/05/28

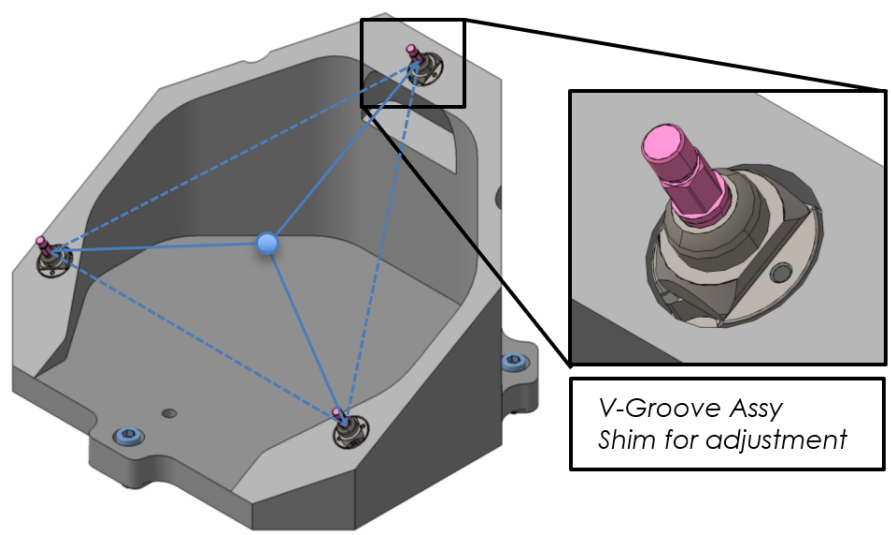

Figure 24. Kinematic mirror mount base - v-grove assembly for adjustment

3.2.2.3 Lens Cell assemblies

Two-piece and monolithic lens cell mounts shown in Figure 25 house larger diameter (>200mm) lenses in the main optical path and calibration leg.

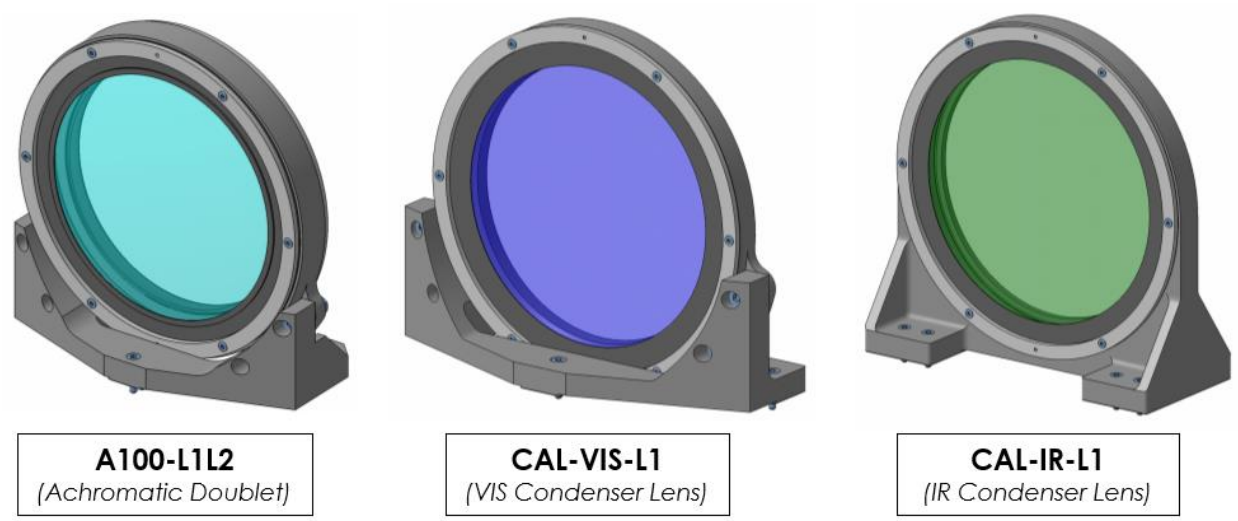

Figure 25. Two-piece and monolithic lens cell assemblies.

Two-piece designs (A100-L1L2 and CAL-VIS-L1) versus monolithic designs (CAL-IR-L1) are needed for the following reasons. Monolithic designs would be a simpler approach however in the case of A100-L1L2, two lenses must be assembled from both sides to create the achromatic doublet so additional base was required. For CAL-VIS-L1, the large diameter lens cell shown previously in Figure 13 is nested in a cutout in the VIS optical bench so the base sits within the clear aperture.

Released 2024/05/28

Released 2024/05/28

Figure 26 depicts typical 304 stainless steel retaining rings clamping the annular flexure rings described in Section 3.2.1.3 on A100-L1L2. The thickness and diameters of the annular flexure rings are tuned for the size and weight of each optic.

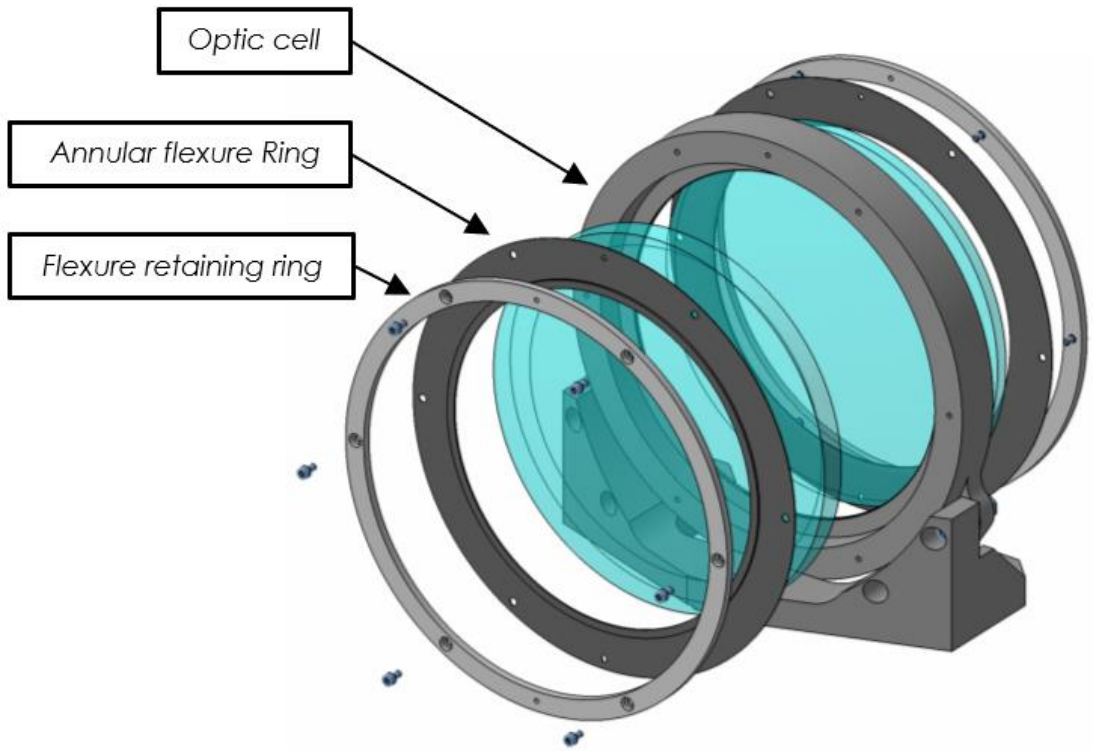

Figure 26. Explode view of A100-L1L2 lens cell assembly.

3.2.2.4 Lens tube assemblies

Custom internally threaded lens barrels are designed to accurately position optics in the A90 IR lens arrays and A110 VIS lens arrays. To meet optical performance parameters, the lens arrays require mechanical support that tightly positions each lens element radially and axially with respect to one another. Where applicable, the convex surface of the lens self-centers about the inner annulus of the spacer or retainer as seen in Figure 27 [3]. If no convex surface is present, a tight 25µm radial gap is maintained between the lens and barrel diameters to minimize misalignment. Figure 28 shows the three unique lens barrel assemblies designed for the IR A90 group and visible A110 group.

Released 2024/05/28

Released 2024/05/28

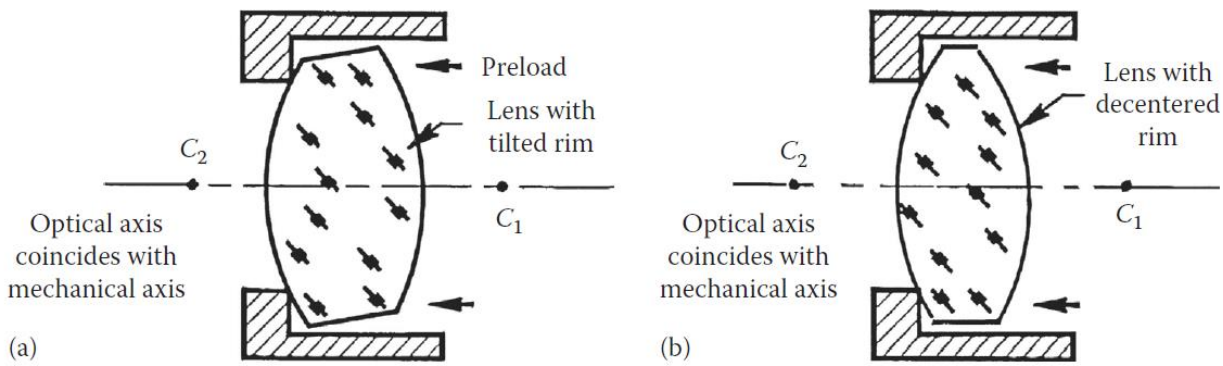

Figure 27. Interface with the polished lens surface negates alignment errors due to (a) tilted rim and (b) decentered rim.

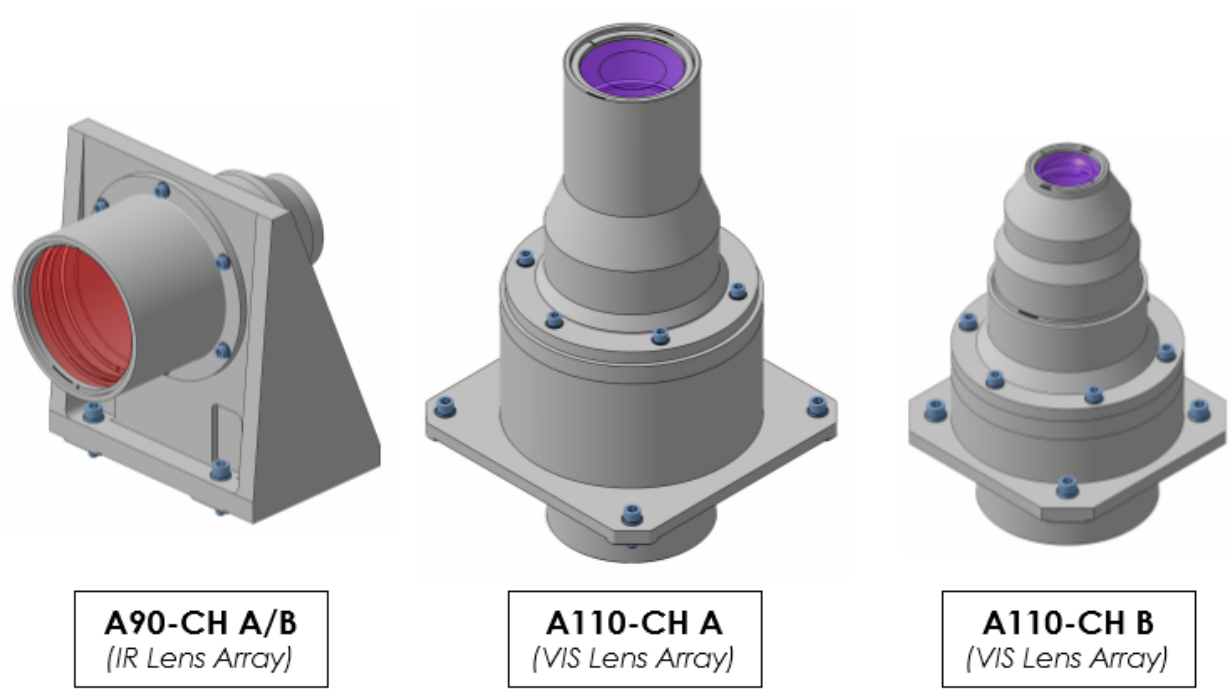

Figure 28. Lens array tube assemblies for IR (A90) and VIS (A110) spectrum bands

Each lens tube assembly is comprised of a 304 stainless steel lens barrel, 304 stainless steel base, and a variety of 304 stainless steel spacers and threaded retainers to position and secure each optic. Each assembly is similar in design, only differing in size and orientation. So, this section of the report will highlight the A90 lens tube assembly.

The lens barrel subassembly (Figure 29) is broken up into a forward (FWD) and AFT section to ease installation of the varying sized optics. The FWD and AFT sections are aligned within +/- 25µm via a pilot guide interface and threaded together. Figure 30 highlights A90 lens barrel pilot guide, M75 threaded interface, and additional gap to shim for axial focus adjustment.

Released 2024/05/28

Released 2024/05/28

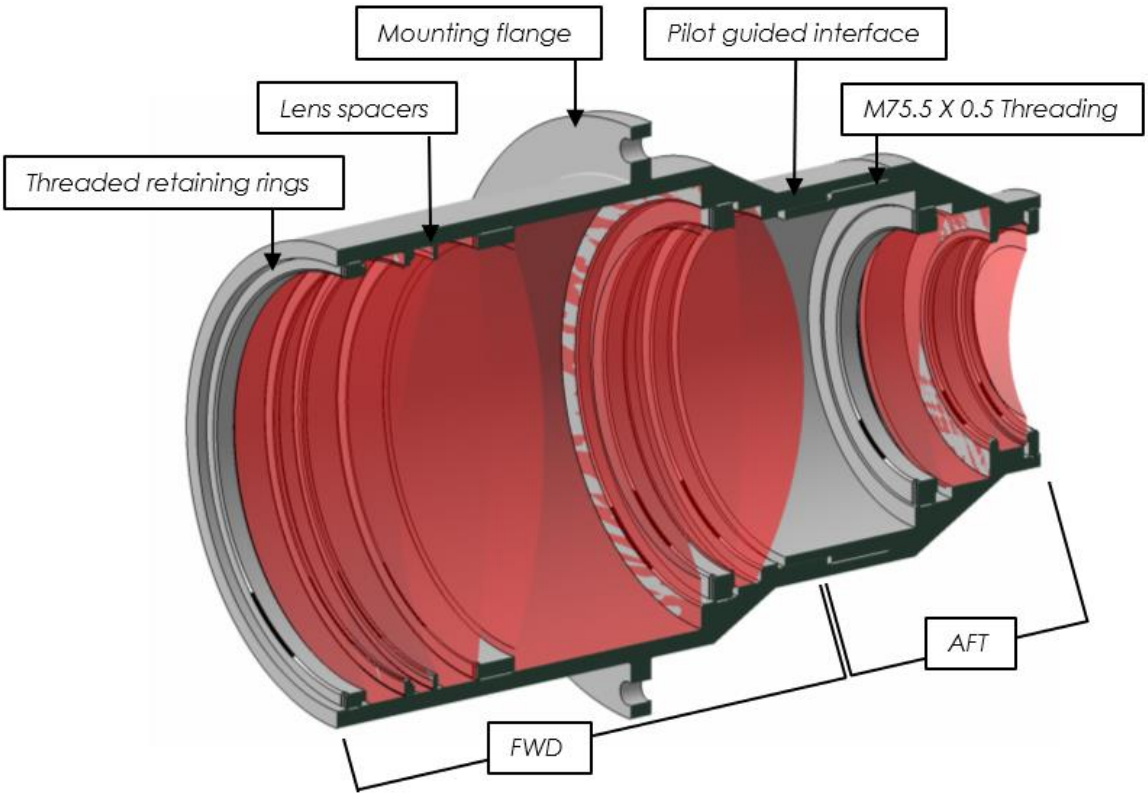

Figure 29. Cross section of A90 IR lens barrel

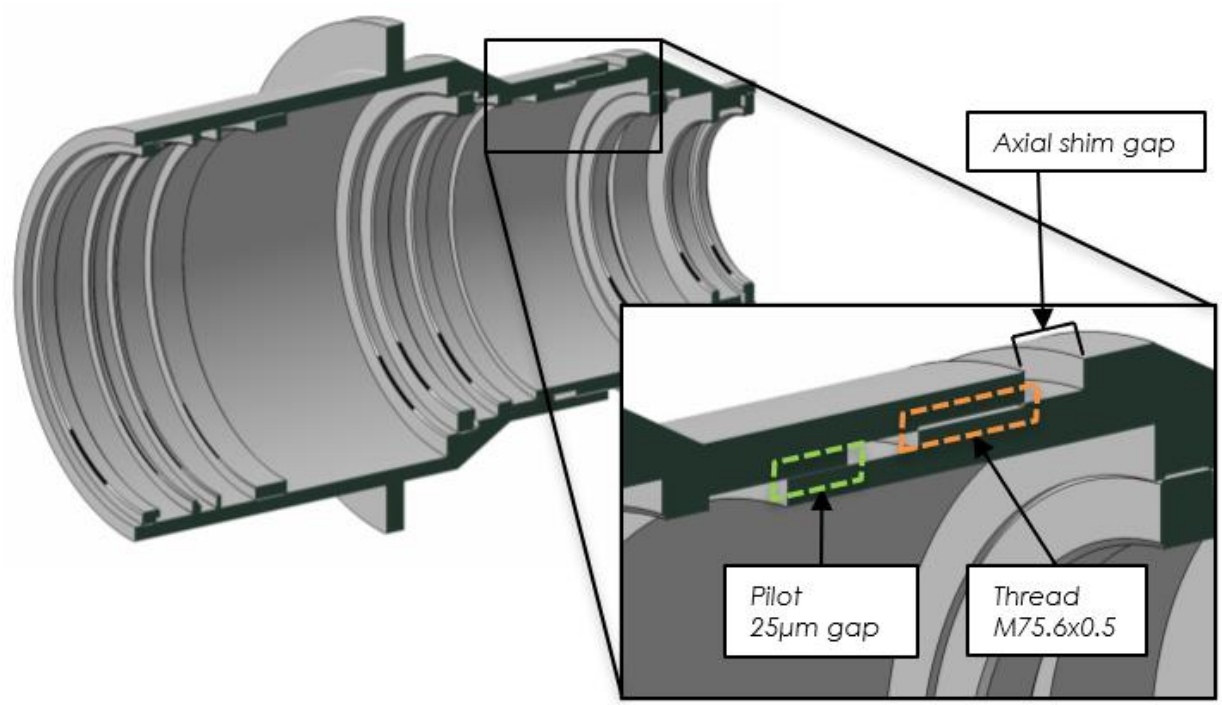

Figure 30. Cross section detail view of A90 lens barrel pilot, threading, and axial shim gap

Released 2024/05/28

Released 2024/05/28

3.3 Visible Filter Wheel Assembly

3.3.1 Design Overview

The filters required to isolate specific visible wavelength bands are mounted in an actuated filter wheel assembly as seen in Figure 31. The filter wheel assembly contains three external tooth filter wheels, a sensor assembly, and three motor assemblies all mated in a two-piece housing. The wheels rotate about a 304 stainless steel shaft and grease free ball bearings.

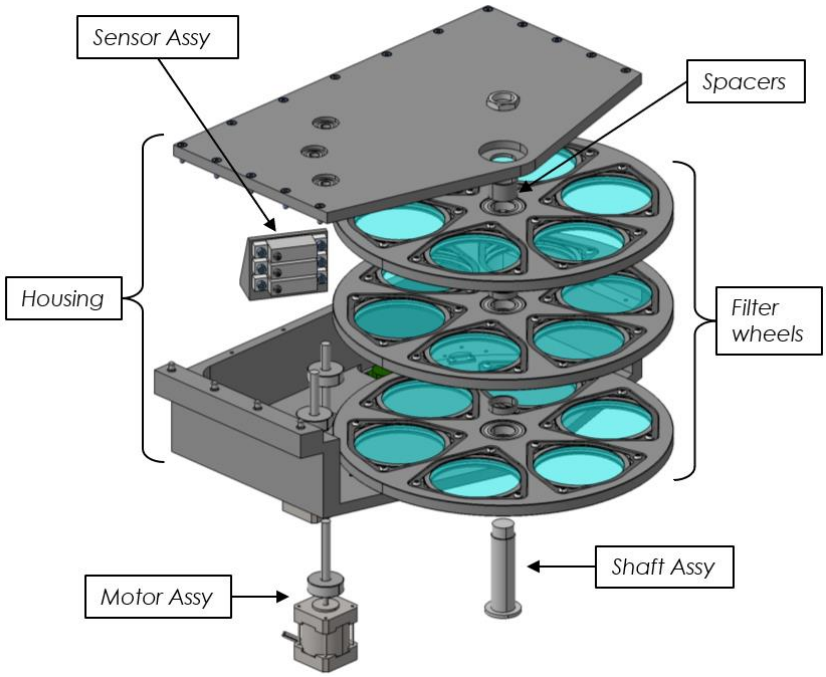

Figure 31. Explode view of visible filter wheel assembly

Three 280mm diameter gears are made from 6061-T6 aluminum and contain six positions for 85mm diameter wavelength and neutral density (Nd) filters. Filters are retained by 17-7 stainless steel flexures which interface with a 6061-T6 aluminum contact pad to reduce optic stresses. Wheel “home” position is indicated by a cam lobe that interfaces with a limit switch assembly. A populated filer wheel is shown in Figure 32.

Released 2024/05/28

Released 2024/05/28

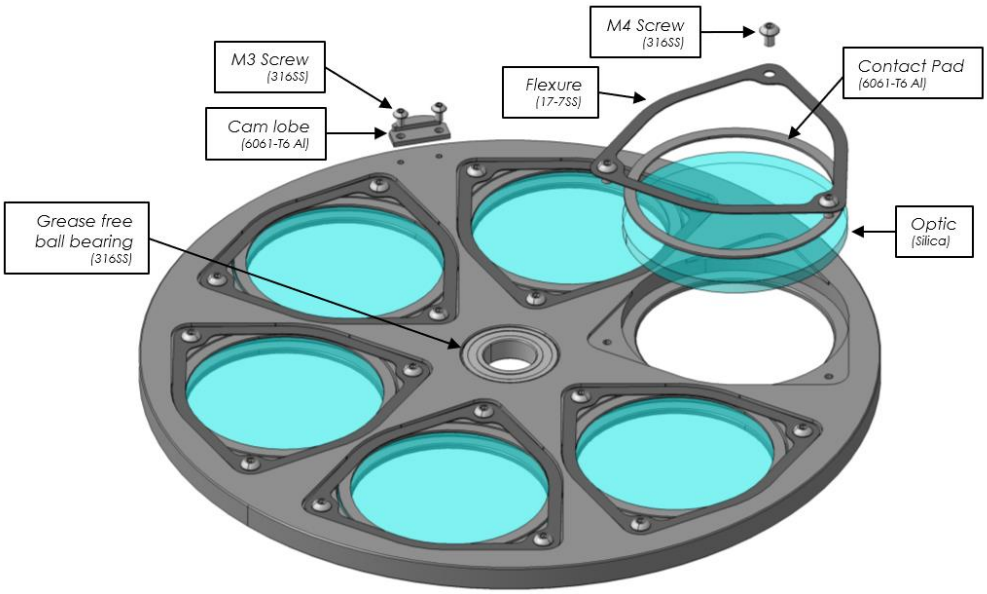

Figure 32. Explode view of populated filter wheel subassembly

Radiation hardened steppers motors drive the filter wheels via 30mm diameter spur gears press fit on a stainless steel shaft (Figure 33a). Radiation hardened limit switches [6] mounted to a 6061-T6 aluminum bracket interface with the cam lobe on each filter wheel subassembly indicating “home” position (Figure 33b).

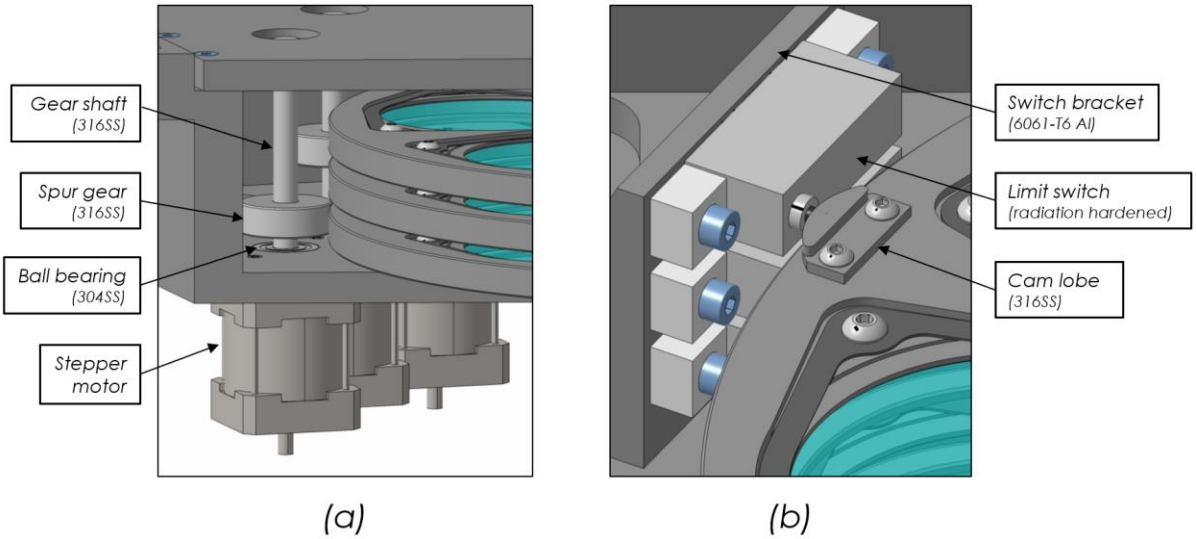

Figure 33. Visible filter wheel assembly (a) motor interface and (b) position sensor interface.

Released 2024/05/28

Released 2024/05/28

3.3.2 Filter Selection Matrix

Preliminary filter wheel position is shown in Table 4. Visible filter wheel selection matrix, with species wavelength lines defined in [7] below.

Table 4. Visible filter wheel selection matrix

Filter Wheel Position	Measurement Parameter										
	H-Alpha Hydrogen	Be Beryllium	W Tungsten	C Carbon	Cu Copper	Ne Neon	Ar Argon	Kr Krypton	He Helium	Thermal	Open
Filter Wheel 3 Wavelength	1	2	3	4	5	6	6	6	6	6	6
	656.1	457.3	400.8	658.2	521.8	Open	Open	Open	Open	Open	Open
Filter Wheel 2 Wavelength	6	6	6	6	6	1	2	3	4	5	6
	Open	Open	Open	Open	Open	640.0	696.5	557.0	728.0	900.0	Open
Filter Wheel 1 Wavelength	TBD	TBD	TBD	TBD	TBD	TBD	TBD	TBD	TBD	TBD	6
	Nd?	Nd?	Nd?	Nd?	Nd?	Nd?	Nd?	Nd?	Nd?	Nd?	Open

3.3.3 Stepper Motor Operation

Radiation hardened stepper motors from Empire Magnetics [8] have been baselined for UWAVS ex-vessel actuation, however due to high radiation activation of cobalt in the motor magnet, modifications to the magnet composition could result in a decrease in performance [9]. Filter wheel operation torque and speeds were calculated in APPENDIX B to be 0.8 in-oz and 3.11 rps respectively and were verified to work with two motor magnetic sizes at 50% power (Figure 34).

Released 2024/05/28

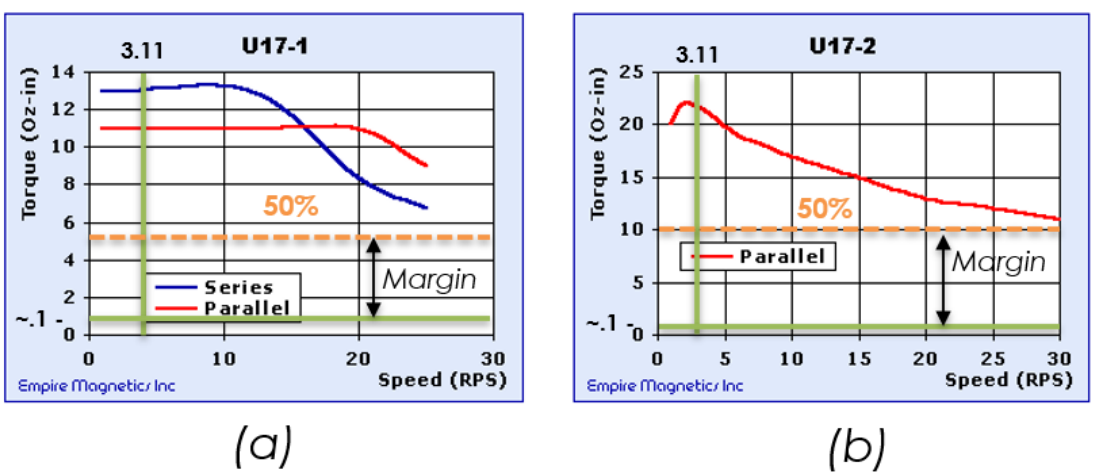

(a) (b)

Figure 34. Stepper motor torque vs speed curves for (a) U17-1 and (b) U17-2 magnet sizes

Released 2024/05/28

3.4 Cameras

The baseline camera selection does not occur until after final design, but a preliminary selection of visible and IR cameras is required for optical and mechanical integration activities. The following camera models were selected for preliminary design.

3.4.1 IR Cameras

For both IR channels A and B, the Infratec ImageIR 9300, water-cooled model was selected. With peak power of 55W and steady state of 27W, water-cooling the camera is necessary to keep it within operating temperatures. The cameras mate with the A90 lens tube assemblies via M60x1 lens interface and are supported by a base to the IR optical bench assembly. Channel A and channel B of the IR optical leg are depicted in Figure 35.

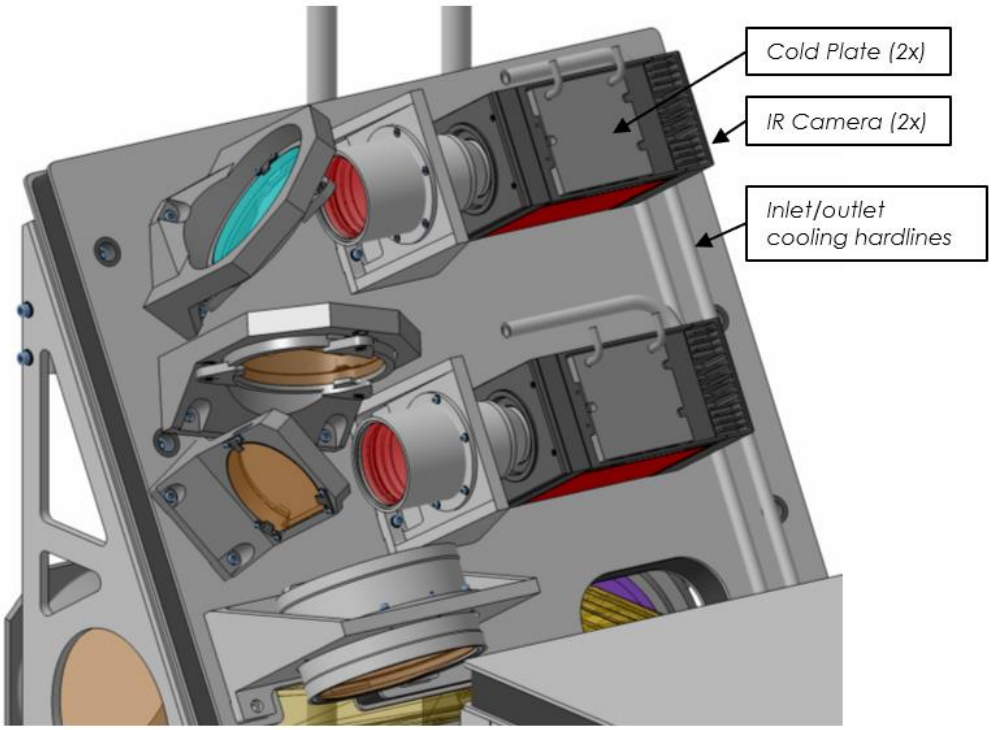

Figure 35. Infratec ImageIR 9300 IR Camera with mounted cold plate

3.4.2 VIS Cameras

Two separate camera models were temporarily selected for visible channels A and B [10]. For channel A the EMV HT-12000 camera was selected for high resolution imaging. For channel B the Mikrotron EoSens 4CPX6 model was selected for high speed capturing.

Thermal analysis indicated a need for focus compensation for both IR and VIS channels due to material CTE of the benches, structures, and optical mounts within each subsystem. A trade study

Released 2024/05/28
Released 2024/05/28

determined that the A40 group of optics in the Interspace Optics Tube (IOT) was most efficient at compensating the IR channel, so VIS compensation had to be performed separately in the BEOC. To account for additional focus compensation, the visible cameras are mounted to stepper motor-driven linear stages affixed to vertical stainless steel mounts. Figure 36 depicts both Channel A and B cameras mounted to the visible optic bench.

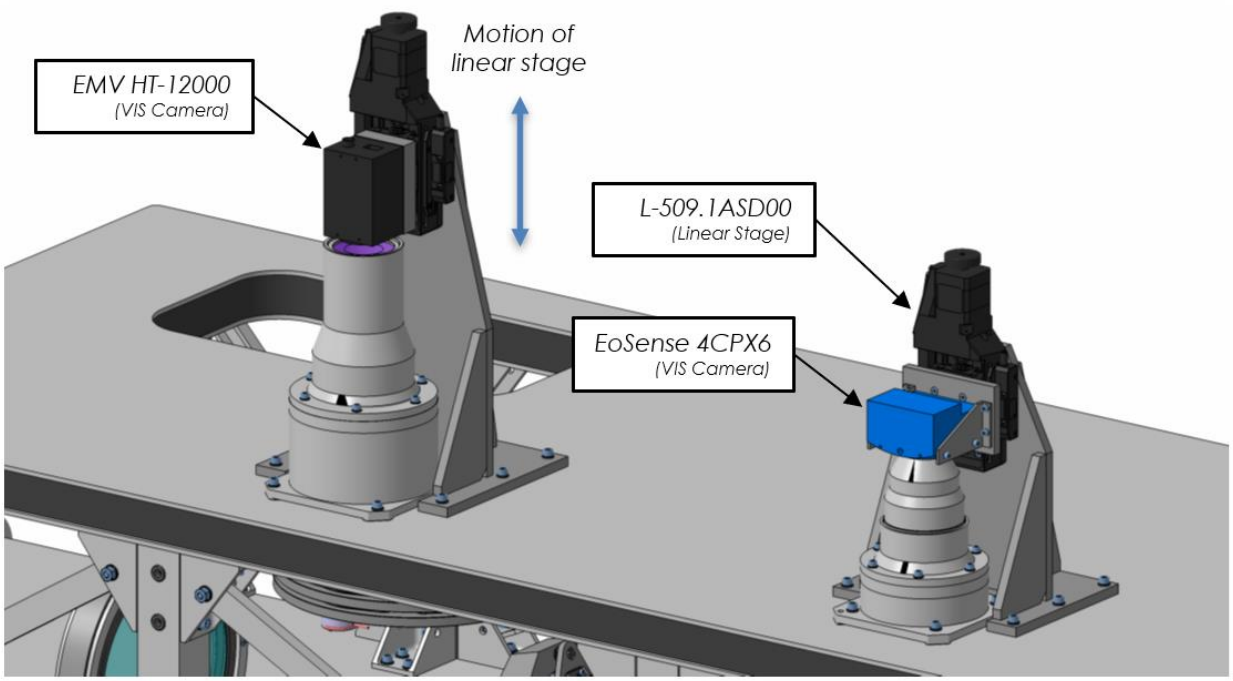

Figure 36. Visible camera channel A and B mounted on linear stages.

3.5 Structures and enclosure

The BEOC structures and enclosures subsystem provides support for optics and instrumentation and protects electronics from the Port Cell environment. Two main assemblies comprise the structures and enclosures which are the optical bench assembly and the shielded cabinet assembly.

3.5.1 Optical Bench Assembly

The optical bench assembly is the main support system for the optics in the optical relay system. The main optical bench, IR optical bench, and VIS optical bench assemble to create the optical bench assembly shown in Figure 37.

Released 2024/05/28

Released 2024/05/28

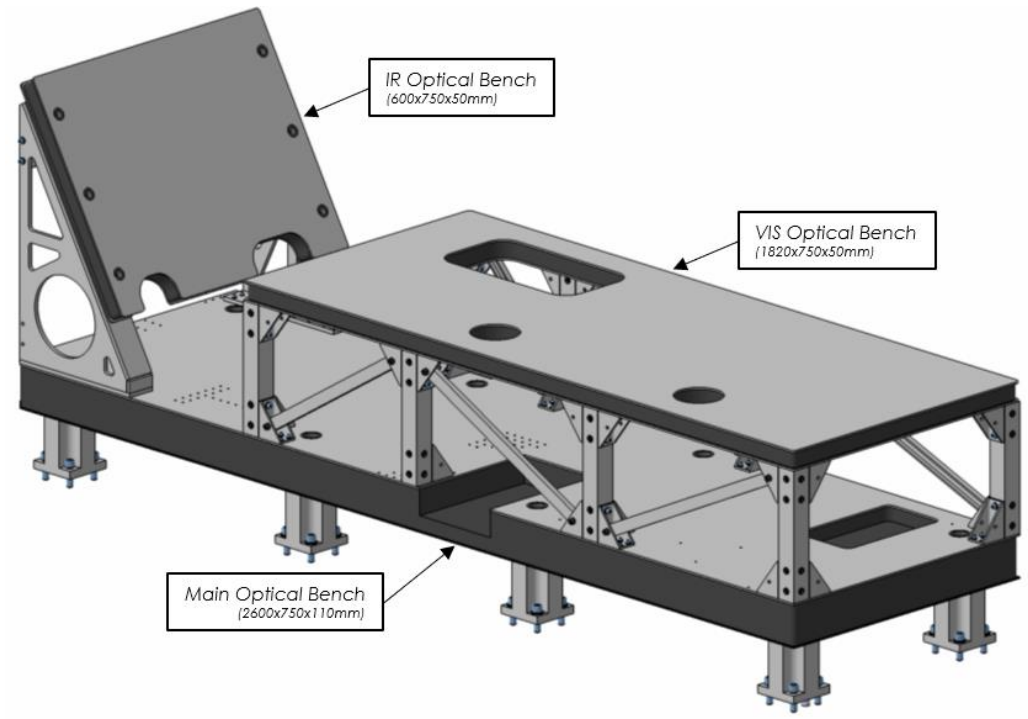

Figure 37. BEOC Optical Bench Assembly

Each optical bench is baselined as a custom Commercial-off-the-shelf (COTS) honeycomb breadboard optical bench. Honeycomb optical benches are industry standard for optical laboratory environments because of their exceptional stiffness, vibration damping, surface flatness, standard threaded hole mounting patterns, and reasonable cost/availability. Standard benches are often configured for more specialized applications, hence the custom-COTS designation. Customized features for each are listed below:

- 316L stainless steel top/bottom sheets and honeycomb core. Edge welded and bonded using radiation compliant materials.
- Pinned interfaces for bench posts, optic mounts, and optical instrumentation.
- Custom threaded inserts for height (dZ), pitch (rY), and roll (rX) adjustment

3.5.1.1 Main optical bench

The main optical bench assembly shown in Figure 38 is the large, lower most bench that provides support to the A70 and A100 optic groups, as well as the IR and VIS optical bench and respective optic groups. The bench itself is a standard 110mm thick bench with a maximum footprint of 2600 x 750mm and standard M6 threaded holes on a 25 mm square pattern. Various levels are recessed into the main breadboard to locate the A100-M2 and CAL-IR-L1 optic mounts in the beam path.

Released 2024/05/28

Released 2024/05/28

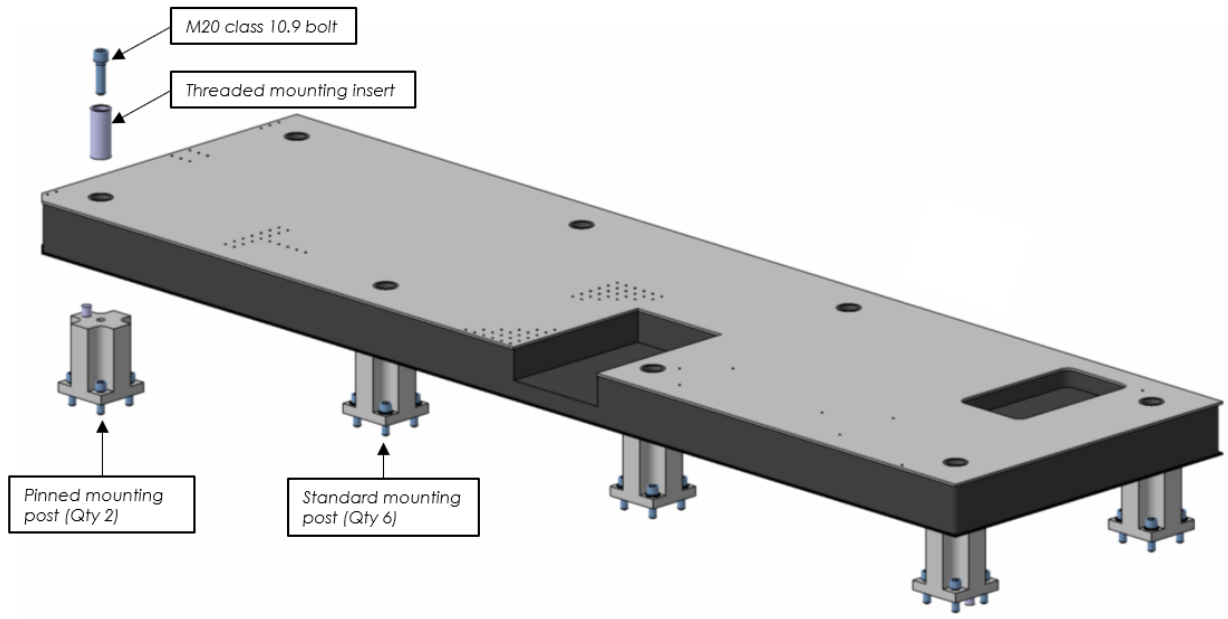

Figure 38. Main optical bench assembly explode view.

The main optical bench is supported by eight 304 stainless steel machined pedestals by M16 and M20 mounting hardware as seen in Figure 39. Two port side pedestals, fore and aft, contain 20mm diameter pins to precisely locate the bench to the lower stainless steel shielding plate. Mounting hardware clamps through a custom insert that's threaded into a welded bushing in the bench similar to Newport Optics Microlock adjuster [11]. This insert shown in Figure 39a allows leveling of the bench.

Released 2024/05/28

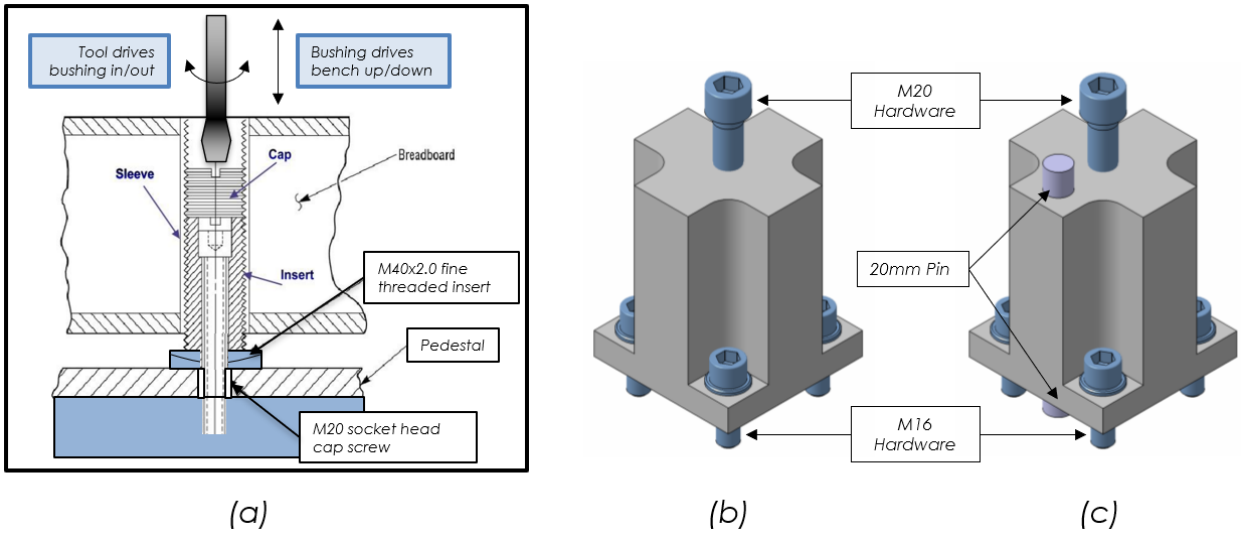

Figure 39. BEOC Main Optical Bench supporting hardware (a) adjustable bushing, (b) standard pedestal, and (c) pinned pedestal.

Released 2024/05/28

3.5.1.2 IR optical bench

The IR optical bench mounts at a 60 degree angle to support the A80, A90, and IR camera assemblies. The bench breadboard is 50mm thick with a footprint of 600 x 750mm and standard M6 threaded holes on a 25 mm square pattern. Similar to the main bench, the IR bench has custom threaded height adjusters to level the assembly with respect to the optical system. Cutouts in the lower portion provide adequate beam clearance for the main beam and calibration beam paths (Figure 40).

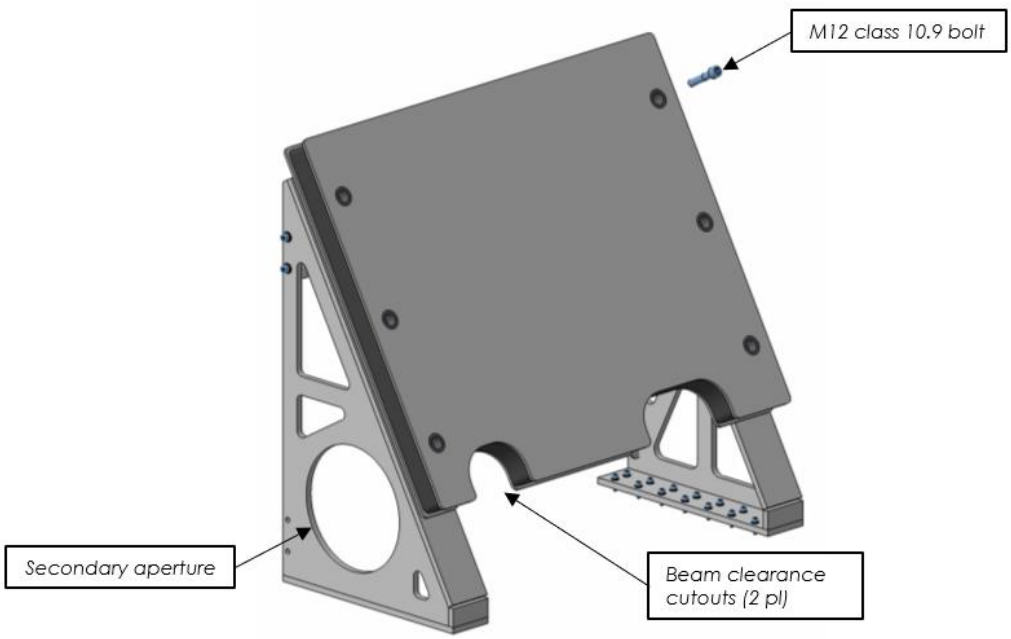

Figure 40. IR bench assembly

The IR bench sits on two welded gussets that mate to the main optical bench by M6 fasteners and positions the IR breadboard at 60 degrees. The port side gusset has a circular aperture to provide the option for a portion of full spectrum light to be directed from A70-S1 to a secondary channel.

3.5.1.3 VIS optical bench

The VIS optical bench is the final optical bench in the BEOC and supports the filter wheels, A110 lens tubes, VIS camera assemblies, and the visible portion of the calibration system. The bench breadboard is 50mm thick with a footprint of 2600 x 750mm and standard M6 threaded holes on a 25 mm square pattern. On the underside are locally positioned M6 fastener holes for the visible filter wheels and mounting posts. Cutouts through the bench shown in Figure 41 allow beam clearance for A110 lens tubes and visible calibration leg.

Released 2024/05/28

Released 2024/05/28

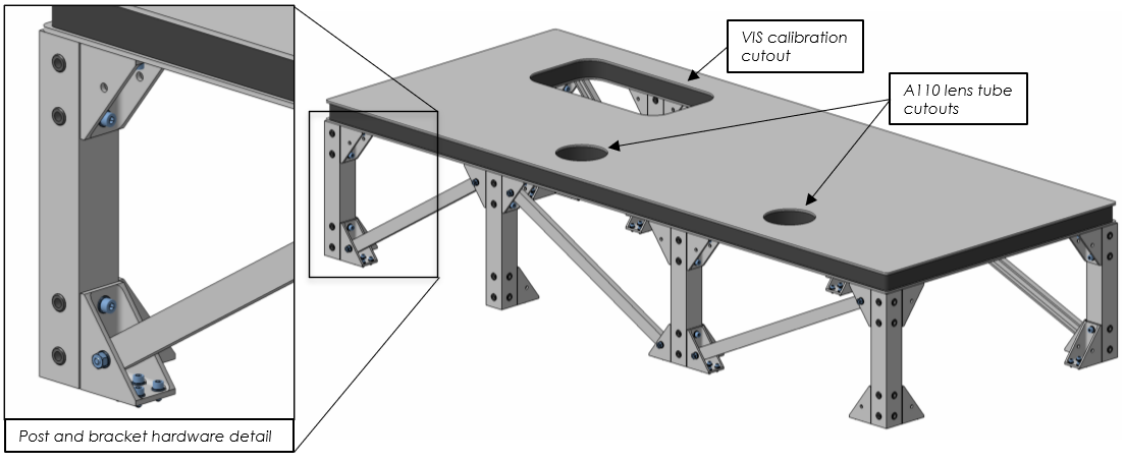

Figure 41. Visible optical bench assembly

The VIS bench is supported by eight 304 stainless steel post and bracket assemblies. The square posts are 325mm tall by 50mm with M8 rivet-nut inserts. Cross supports between the vertical posts bolt to the angle brackets with M8 hardware.

3.5.2 Shielded Cabinet Assembly

The shielded cabinet assembly provides two main functions: To protect BEOC electronics from radiation and magnetic loads, and to protect optics from dust ingress from the Port Cell. The primary components of the shielded cabinet assembly are the shielding layers and maintenance doors as shown in Figure 42.

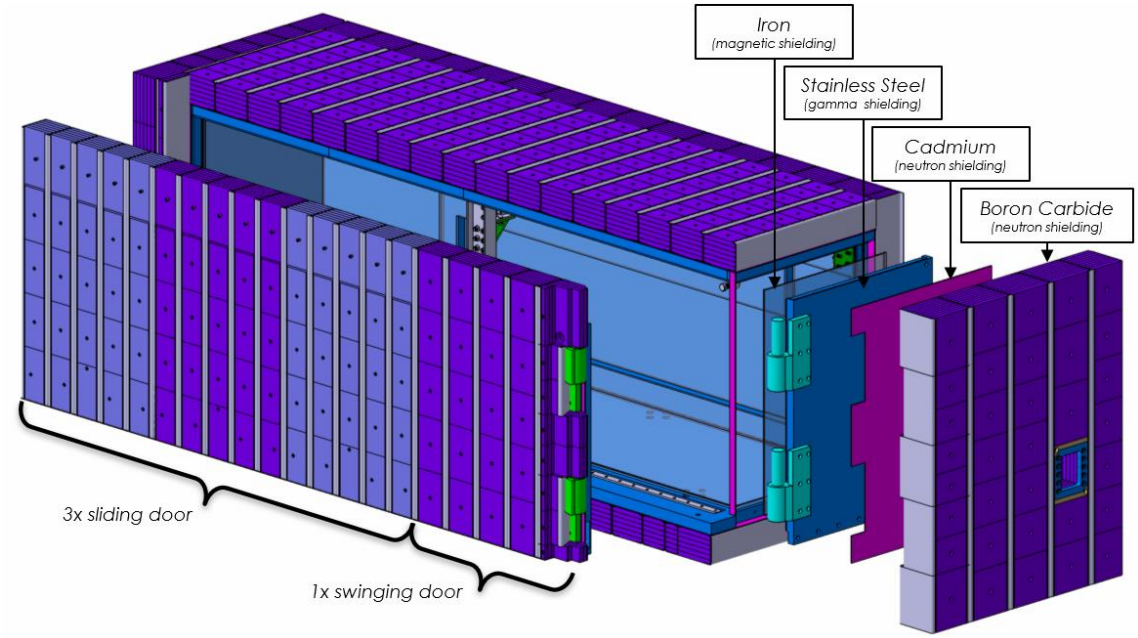

Figure 42. Explode view of shielded cabinet assembly components.

Released 2024/05/28

Released 2024/05/28

3.5.2.1 Shielding

The primary function of the shielded cabinet assembly is to attenuate both radiation and magnetic loads in the port cell to protect sensitive equipment in the BEOC assembly. Layers of magnetic, gamma, and neutronic shielding materials are stacked and assembled to create an enclosure to accomplish this task. Shielding layers, thicknesses, and retention methods are heavily based on 55.G1 (EWAVS) shielded cabinet assembly [12].

3.5.2.1.1 Gamma shielding

A 60mm thick layer of 316 stainless steel provides the required gamma radiation attenuation. Due to the strength and stiffness of 316 stainless steel, the gamma shielding also functions as the primary structure of the shielded cabinet assembly. The stainless steel structure in Figure 43 has cutouts for bench clearance, mounting points for optics and the optical bench assembly, tracks and hinges for maintenance doors, as well as fixation points for subsequent shielding layers. Laterally across the center spans an I-beam assembly, comprised of 5inch I-beams and gussets, to support the top stainless steel plates at their joint.

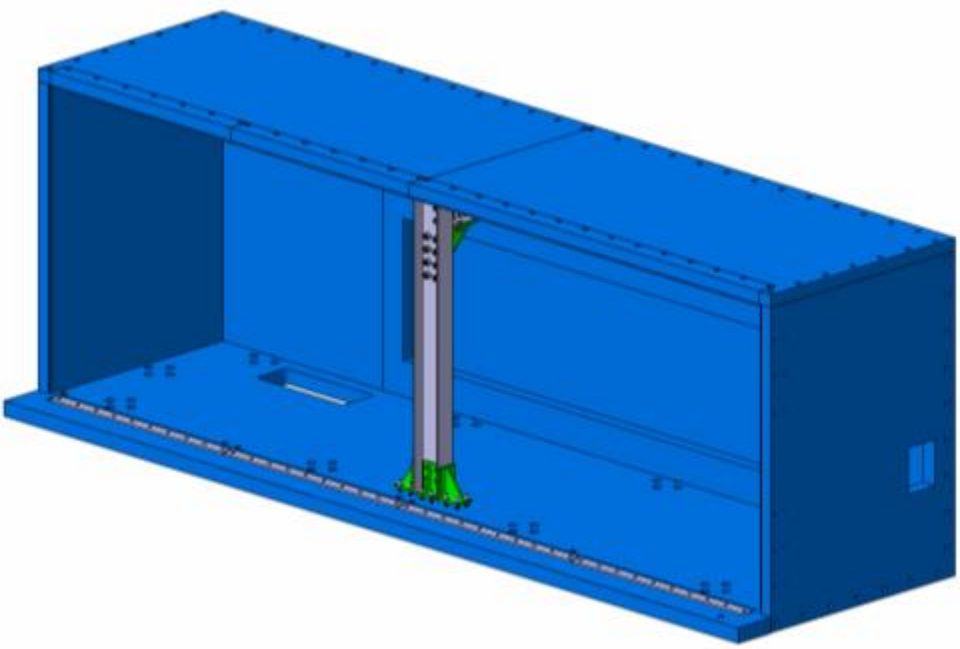

Figure 43. Stainless steel gamma shielding structure.

The optical beam path is favored towards the port side of the BEOC so local gamma shielding in Figure 44 is shifted to provide clearance for the optical bench assembly and various optics. To accomplish this, shielding is removed locally and a 2772mm x 912mm plate bolts to the port side. Aside from providing clearance, the cutout allows additional access to the port side of the optical bench assembly during factory installation and testing.

Released 2024/05/28

Released 2024/05/28

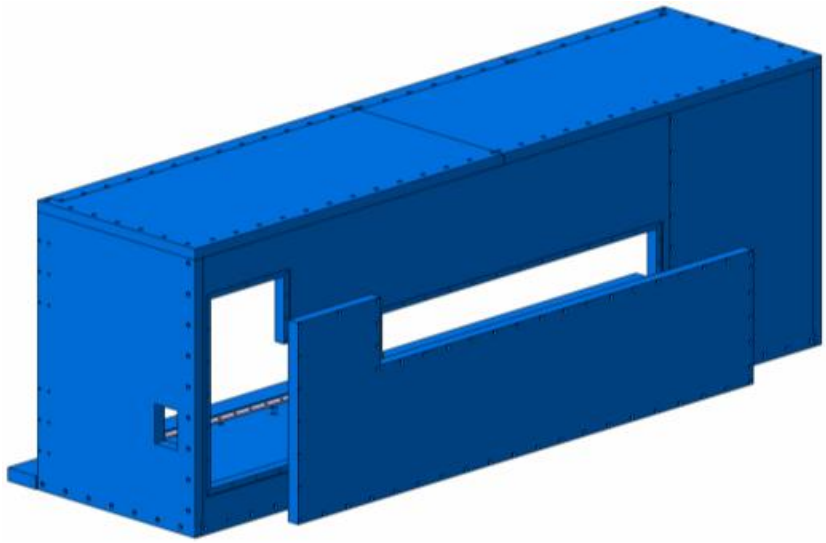

Figure 44. Port side shifted gamma shielding for clearance and access.

3.5.2.1.2 Neutron shielding

The outermost layer of the shielded cabinet is comprised of stacks of 25mm thick boron carbide (B4C) plates to attenuate neutron radiation to acceptable levels. Pre-assembled B4C bricks slide into 316 stainless steel C-channels bolted to the shielded cabinet as seen in Figure 45. In addition to B4C, a 5mm layer of neutron absorbing cadmium is mounted under the stainless steel channels.

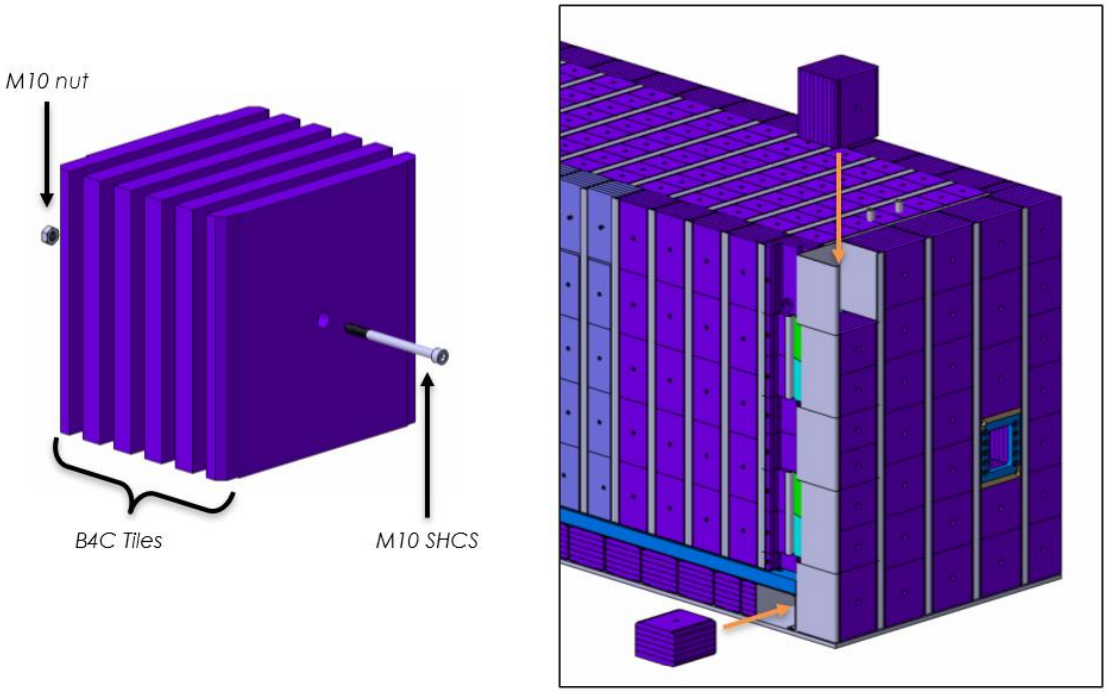

Figure 45. Neutron shielding B4C brick and assembly into rail channel system.

Released 2024/05/28

Released 2024/05/28

3.5.2.1.3 Magnetic shielding

Magnetic shielding is accomplished using a 15mm thick layer of pure iron. The iron layer creates an inner shell when mounted to the inner surface of the stainless steel structure. Various cutouts shown in Figure 46 allow service access and optical bench and beam clearance.

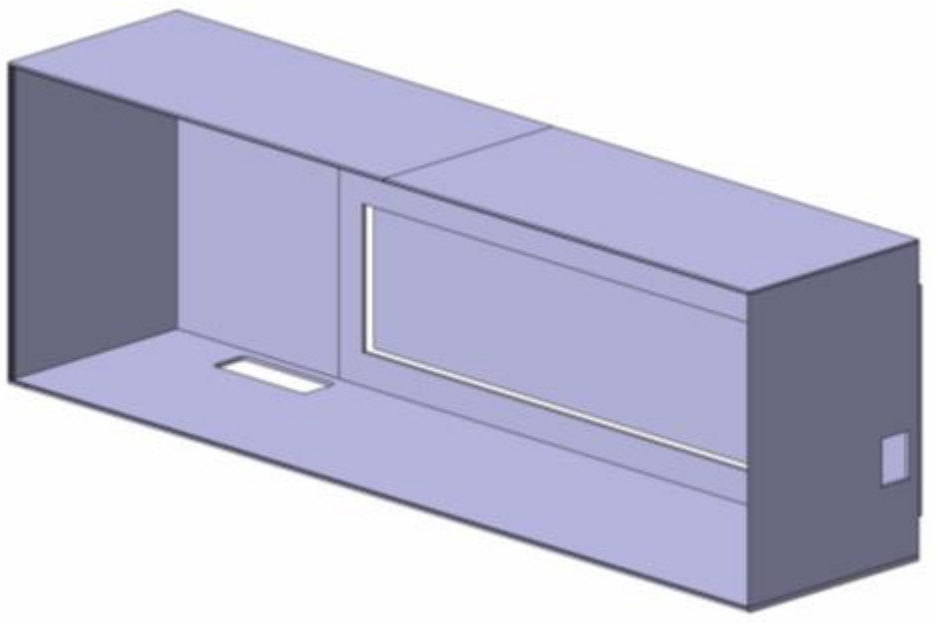

Figure 46. Magnetic iron shielding layer.

3.5.2.2 Maintenance doors

To facilitate maintenance to BEOC optics and electronics, a front swinging door followed by a series of three sliding doors operate in series to allow access by personnel. Shielding compositions and thicknesses on the maintenance doors are consistent with the rest of the shielded cabinet assembly.

The front swinging door weighs 1275kg and mounts to the forward stainless steel panel via two industrial hinges rated to over 11000kg each. The three rolling doors weigh 1125kg and are supported by three bottom casters rated for 1900kg each. To prevent the sliding doors from tipping outwards, an assembly with six horizontal rollers bolts to the top of the door and tracks through a longitudinal guide in the top stainless steel structure. Detail views of the maintenance door hinge and caster/roller assemblies can be found in Figure 47.

Released 2024/05/28

Released 2024/05/28

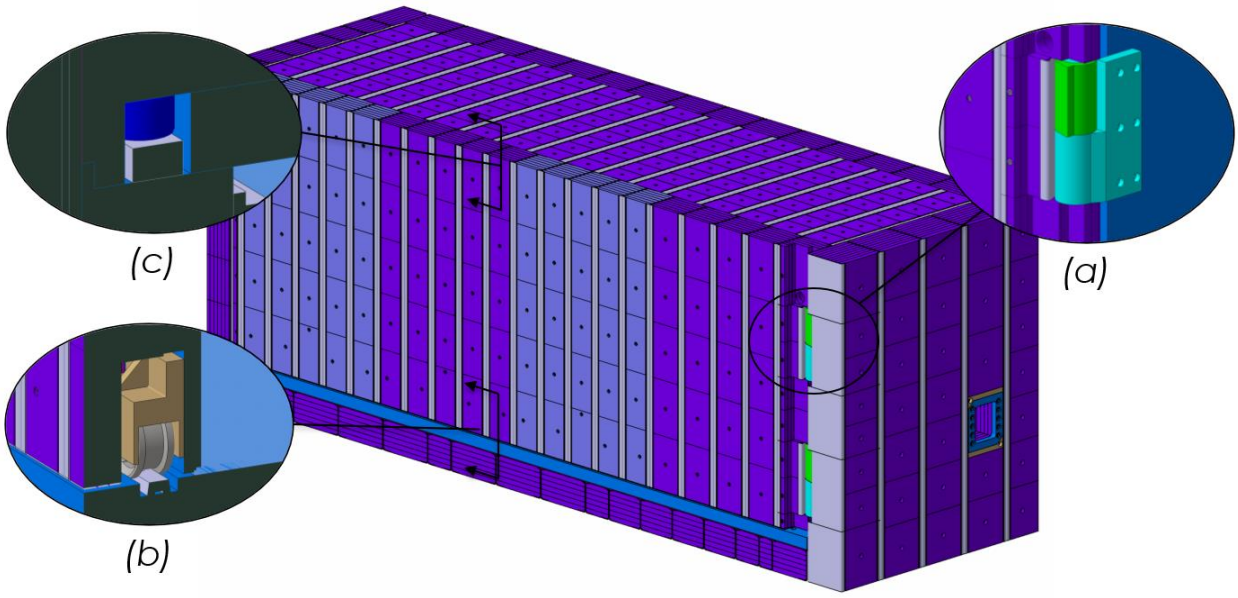

Figure 47. Detail views of (a) front industrial hinge, (b) bottom caster assembly, and (c) top roller assembly.

As previously mentioned, the maintenance doors operate in series to provide access to personnel. First, the front swing door must be opened to its full extent and locked in place, exposing the IR optical bench and cameras. Next the first sliding door can be rolled forward, butted up to the first swing door, thus providing access to the VIS calibration optics and first visible camera assembly. In a similar fashion, the remaining sliding doors can be rolled forward giving access to the second visible camera assembly and calibration sources. An overview of maintenance door operation is highlighted in Figure 48.

Released 2024/05/28

Released 2024/05/28

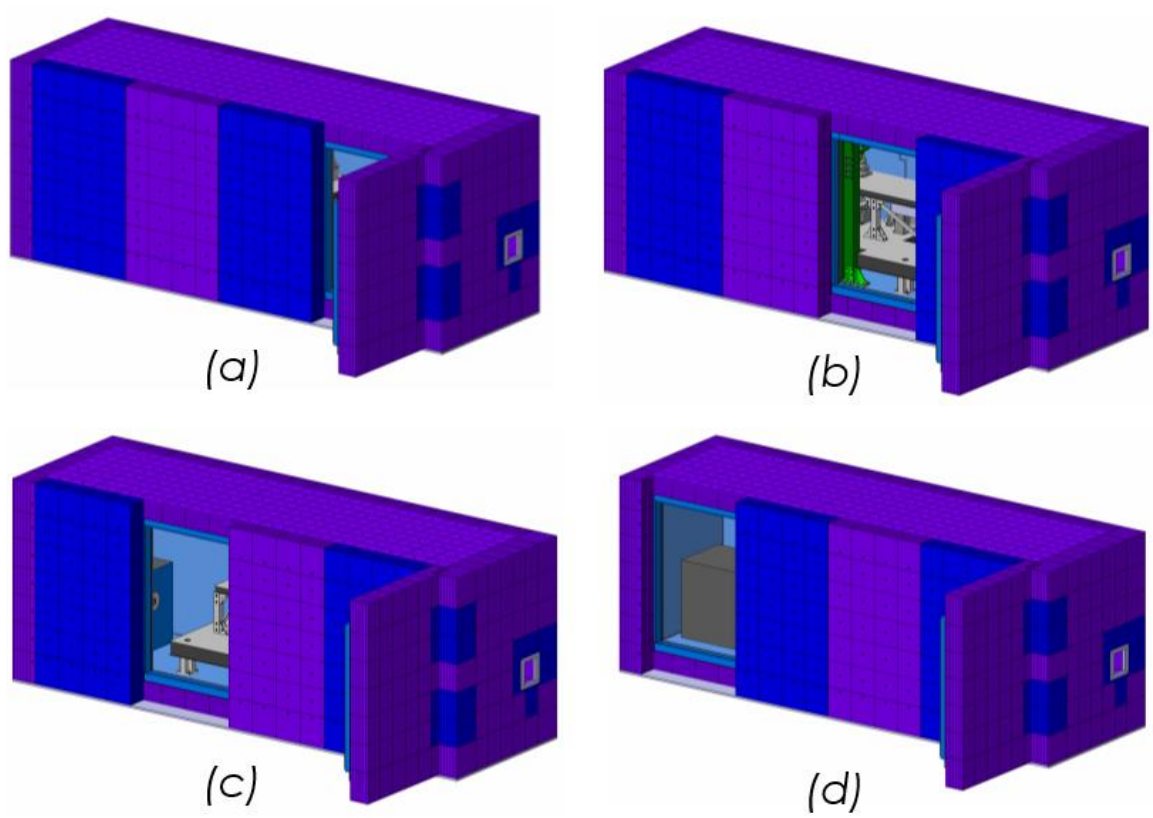

Figure 48. BEOC maintenance door operation (a) first front door swings open, (b) second sliding door, (c) third sliding door, and finally (d) fourth sliding door.

To lock doors in place during operation and for safety while under maintenance, a variety of pins and bolts are located in the stainless steel structure to secure doors in different positions. Each sliding door has two positions for a locking pin at the forward and aft bottom of the steel layer. When the sliding door is moved into position, a 20mm pin is inserted downwards through the door and into a hole in the bottom stainless steel track, locking it into position. This process can be performed at any location the door can reside, locking the door safely into position for maintenance or locking it closed for operation. Similarly, the front swinging door has one location at the forward bottom of the steel layer for a locking pin. The 20mm locking pin for the swinging door is only used to lock the door open for safety during maintenance. Finally, to close all doors for operation, all sliding doors are rolled into position with pins installed and the front swinging door is locked closed by a M24 bolt through the door into the structure. Details of both bolted connections and pin locks are shown in Figure 49.

Released 2024/05/28

Released 2024/05/28

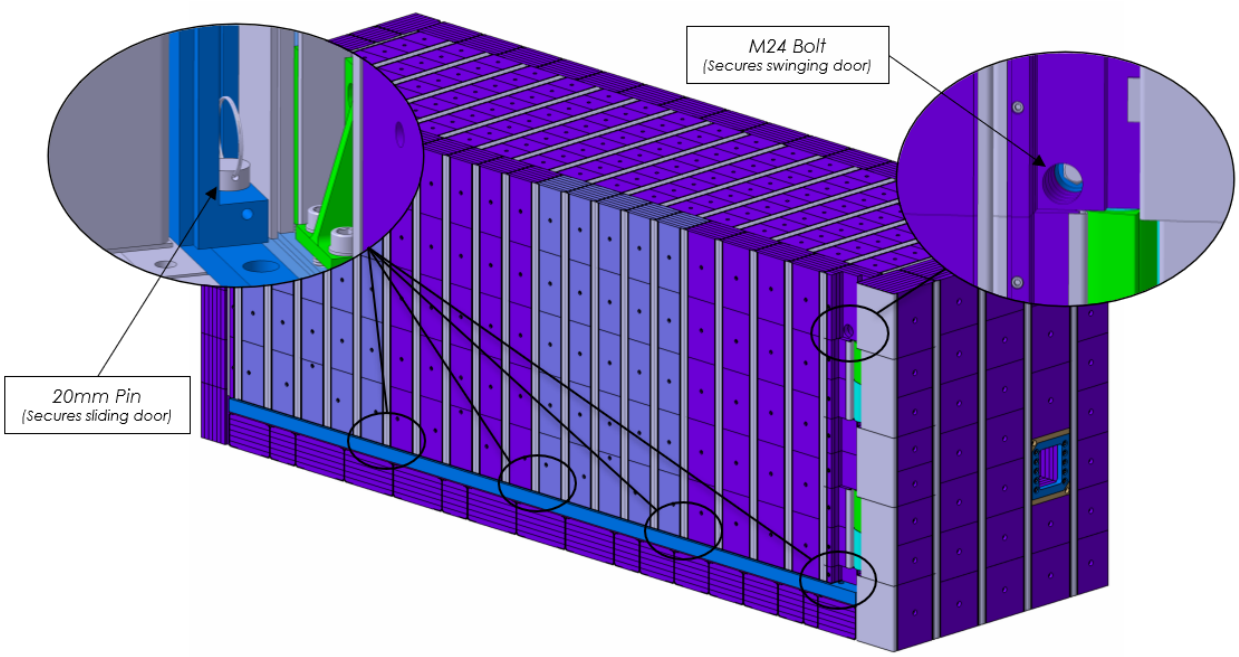

Figure 49. BEOC shielded enclosure locking detail views.

3.6 BEOC Interfaces and Services

This section provides a brief, high-level summary the BEOC subsystem external interfaces and service requirements. Detailed interface descriptions and associated data can be found in the following interface sheets (IS):

- 55.GA IS for UPP-02 [13]
- 55.GA IS for UPP-08 [14]
- 55.GA IS for UPP-11 [15]
- 55.GA IS for UPP-14 [16]

BEOC interface and service components facilitate delivery of general services from the Upper Port Cell support structure to internal BEOC components, and provides other auxiliary functions to support installation, removal, and maintenance of the BEOC subsystem and its components. The baseline design of the BEOC requires power and signal services to electrical components and cooling services to the IR cameras and IR calibration source.

3.6.1 Interface plate

The BEOC interface plate assembly facilitates the interface between the BEOC and the Port Cell Support Structure (PCSS). The BEOC interface plate assembly also provides initial installation alignment/correction to overcome significant absolute installation tolerances of the PCSS per [17]. The BEOC interface plate assembly consists of the following components, as shown in Figure 50.

Released 2024/05/28

Released 2024/05/28

- BEOC interface plate – 55.GA defined in Port Integrator (PI) interface sheet.
- Interface plate pucks and hardware.
- Welded hardware [18] for BEOC enclosure pedestals.

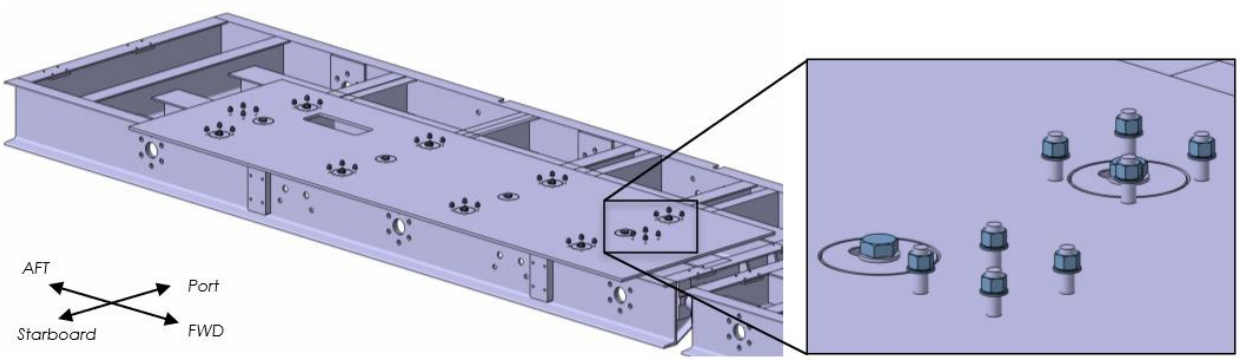

Figure 50. BEOC interface plate mounted on PCSS with detail view of puck and pedestal hardware.

The interface plate pucks secure the BEOC interface plate to the PCSS using M20 bolts and Wedgelock washers [19] in an oversized slot, as shown in Figure 51. Translation of the bolt shank in the slot, combined with rotation of the puck in the interface plate counterbore allow for planar (local XY) alignment of the BEOC interface plate assembly during initial installation.

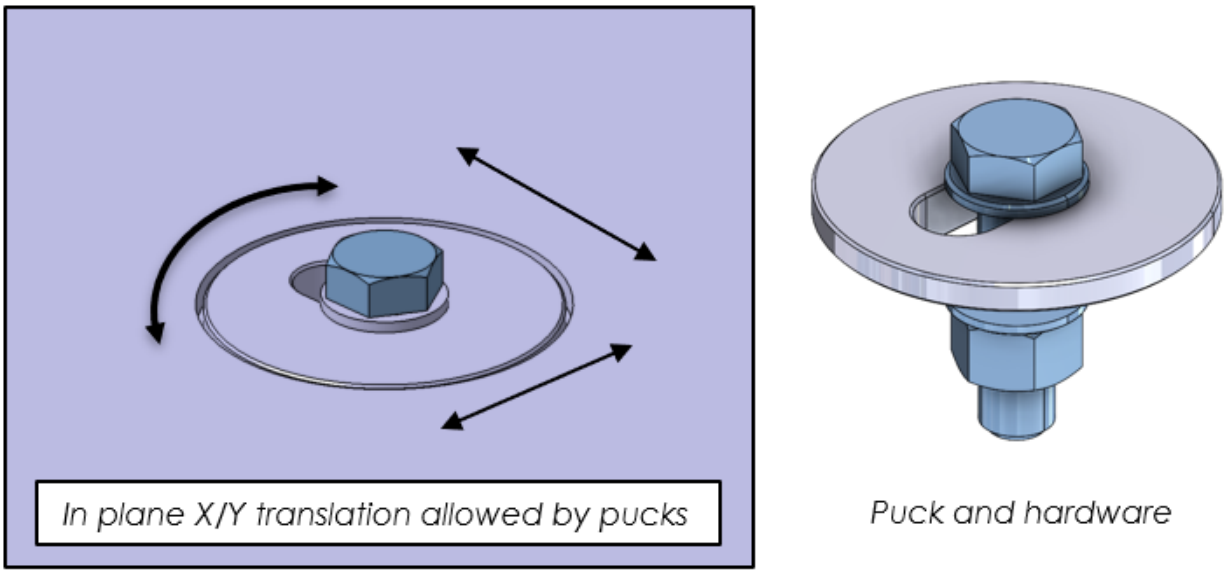

Figure 51. BEOC interface plate alignment pucks facilitate X/Y in plane translation.

Released 2024/05/28

Released 2024/05/28

The optical bench posts mount upon the M16 weld-on studs of the interface plate using hex nuts and Wedgelock washers. Two configurations of posts are required, with one configuration containing press-fit precision locating pins to mate with the 20 mm pinholes on the interface plate, as well as pinholes on the BEOC shielded enclosure.

At the bottom side of the posts a 5 mm shim stack is nominal. This shim stack allows for +/- 5 mm coarse vertical (TGCS Z-direction) adjustment during initial installation. At the topside of the posts are M20 helical threaded inserts to accept the mating bolts from the BEOC shielded enclosure.

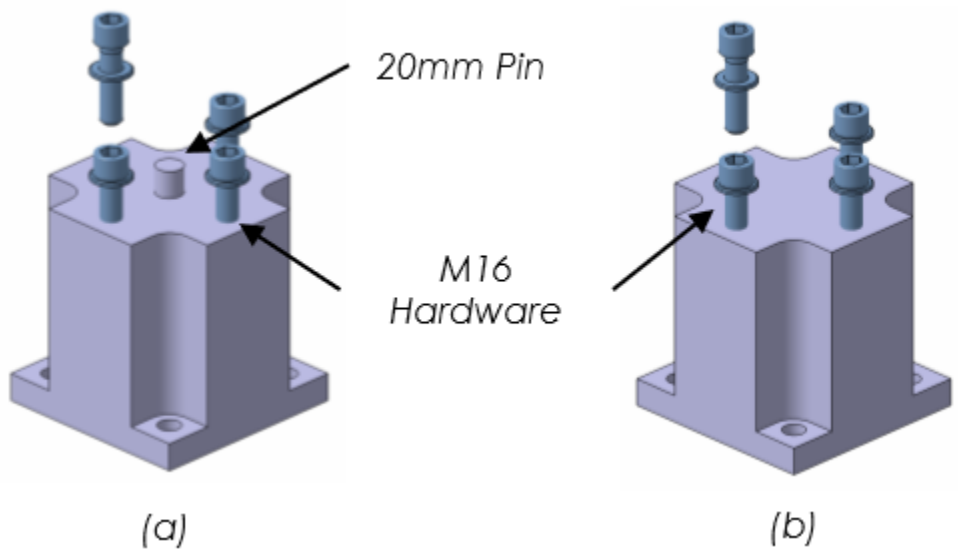

Figure 52. BEOC enclosure pedestals with (a) pinned interface and (b) standard interface.

3.6.2 Electrical services

The BEOC electrical service system is broken out into three sections highlighted in Figure 53 below:

1. BEOC internal cable routing (55.GA scope)
2. BEOC intermediate adapter cable (55.GA scope)
3. PCSS external cable routing (Port Integrator scope)

Released 2024/05/28

Released 2024/05/28

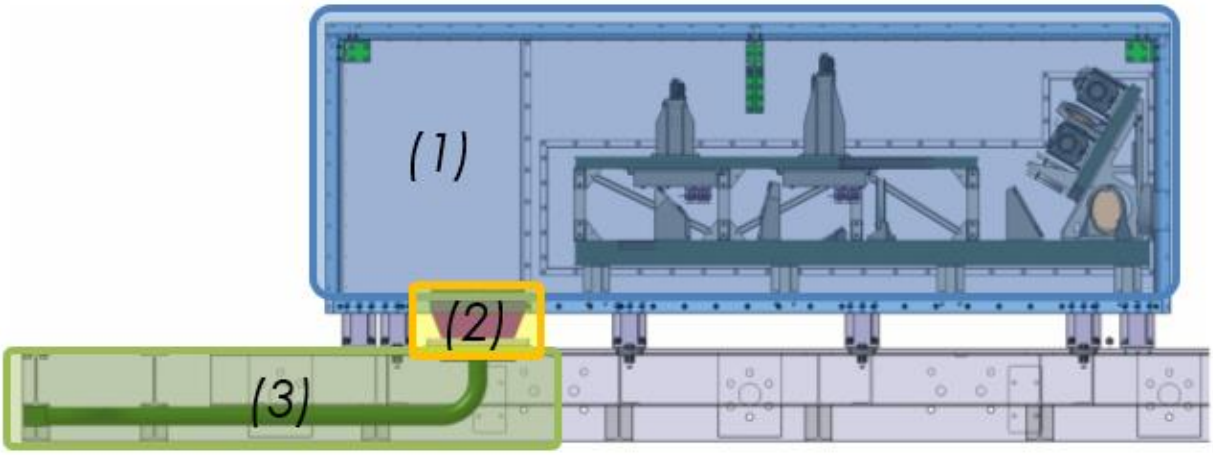

Figure 53. BEOC electrical service system (1) internal cable routing (2) intermediate adapter cable and (3) PCSS external cable routing.

The BEOC internal cable routing brings electrical power and signal to the various instrumentation in the shielded enclosure. Cables route from a bulkhead assembly (Figure 54) at the aft port side base and route to the IR cameras, visible cameras and linear stages, filter wheel assemblies, calibration sources, as well as required thermocouples and sensors. Cables will be segmented so disconnects will be located close to equipment for ease of maintenance.

The intermediate adapter cable shown in Figure 54 passes power and signal through the various shielding layers from the PCSS interface plate. In addition, the cable serves as an adapter by taking the external Staubli cable connector [20] and breaking it up into discrete circular connectors [21] for equipment specific cables.

The external cabling passes along the underside of the PCSS from a bulkhead located on the BEOC interface plate assembly. In Figure 54, a disconnect at the AFT PCSS represents the Port Cell service connector.

Released 2024/05/28

Released 2024/05/28

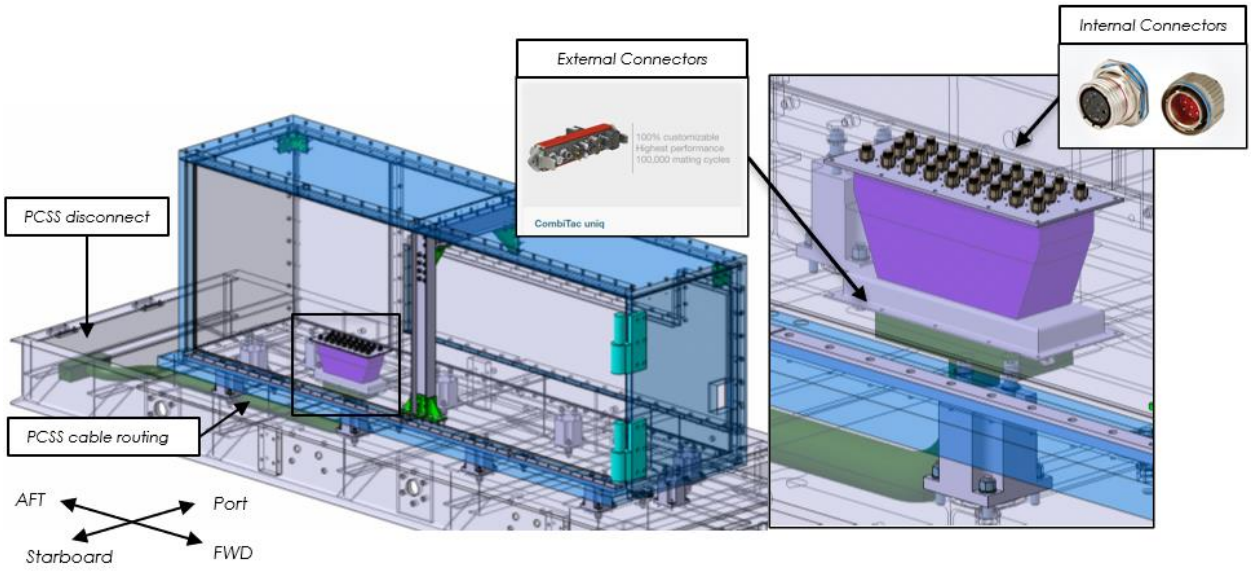

Figure 54. BEOC electrical service disconnects for internal, external and PCSS locations.

Cabling diagrams are listed below for reference.

- 55.GA CBD for UPP-02 [22]
- 55.GA CBD for UPP-08 [23]
- 55.GA CBD for UPP-11 [24]
- 55.GA CBD for UPP-14 [25]

3.6.3 Cooling services

Cooling services from Component Cooling Water Supply (CCWS) and Chilled Water Supply (CHWS) interface with tube studs at the forward top portion of the BEOC as seen in Figure 55. Cooling pipes drop down the front iron wall and then route back along the bottom of the enclosure under the main optical bench assembly towards the IR calibration source. Water is directed upwards along the main and IR optical benches by stainless steel pipes before coupling to stainless steel braided flexible lines for the IR camera cold plates (Figure 55).

Conditioning between loops to tune cooling water to optimize IR camera and source performance may be implemented. This could be conducted via a water-to-water heat exchanger and actuated throttling valves.

Released 2024/05/28

Released 2024/05/28

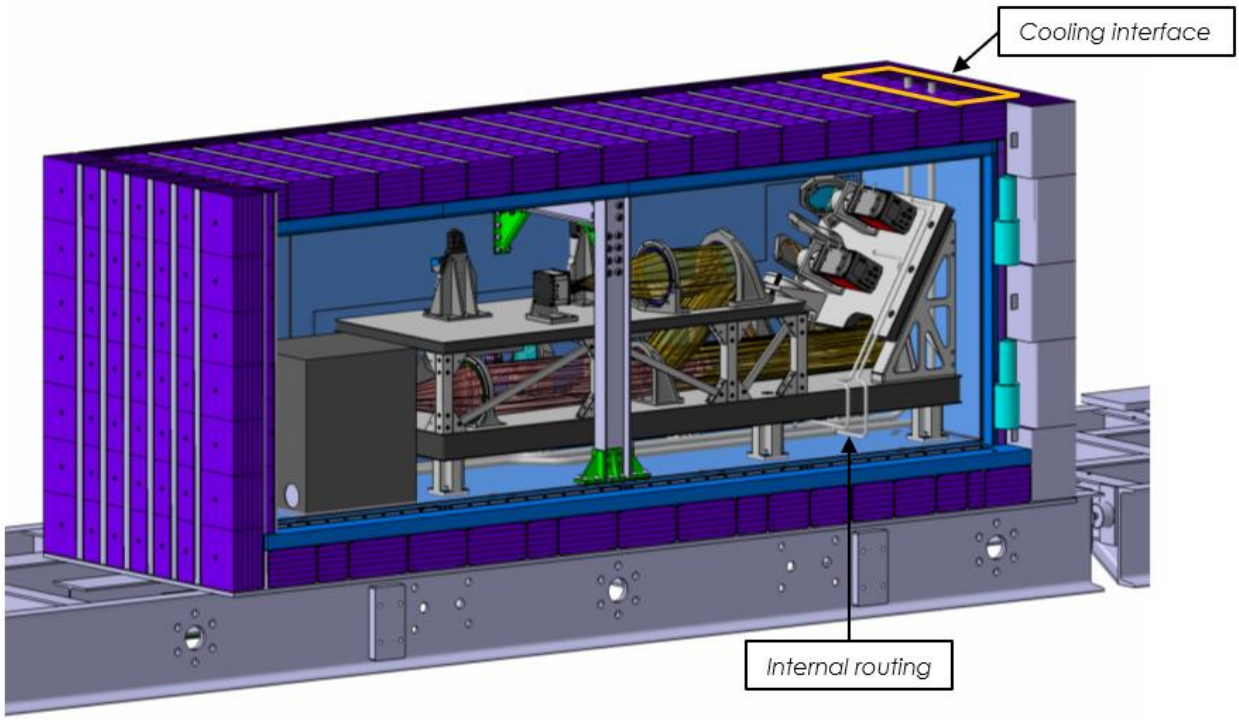

Figure 55. BEOC cooling services interface at FWD top and internal routing to equipment.

3.6.4 Beam Shrouds

A telescoping beam shroud in Figure 56 mounts between the BOL and the front of the BEOC enclosure to protect the diagnostic line of sight from contamination and stray light as it passes between 55.GA subsystems. The beam shroud is designed to provide adequate beam path clearance between the BOL and BEOC. Detailed design of the beam shroud is covered in the Bio-shield Labyrinth (BOL) technical design description [26].

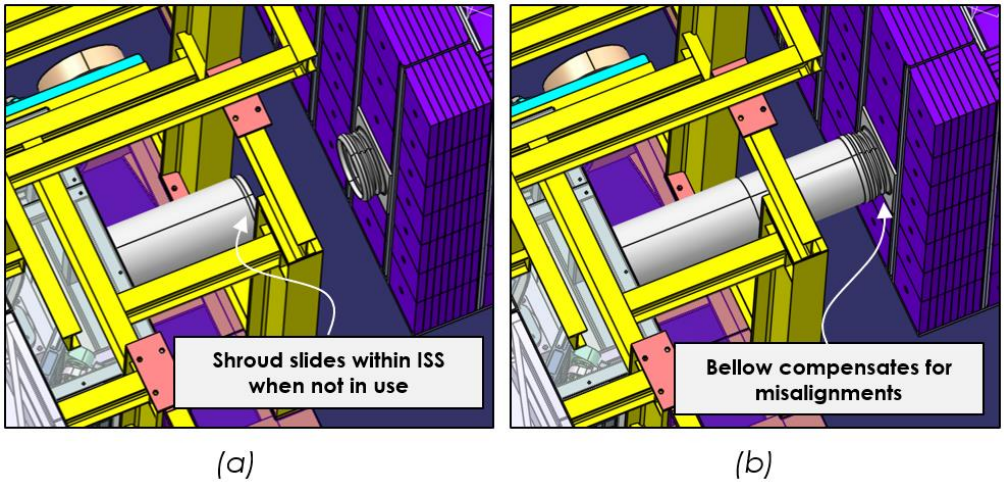

Figure 56. BOL to BEOC beam shroud (a) telescoping section and (b) bellow.

Released 2024/05/28

Released 2024/05/28

3.6.5 Secondary Channel

In the baseline preliminary design, roughly 10% of full spectrum light can be directed out of the port side of the BEOC via the A70-S1 splitter to a secondary channel. Currently there is no optical window on the port side of the enclosure, so a pneumatic shutter may be needed to keep dust and contamination out when not in use. Alternatively, a fiber bundle may be used to capture and direct light outside of the BEOC enclosure. If this is the case, the aperture in the shielding will be sized appropriately so that the fiber bundle will completely plug the hole. In final design, a fiber bundle, window, or shutter will be evaluated.

Although light can split within the BEOC, it is recommended in final design that light be directed for the secondary channel forward of the BEOC due to space constraints within the enclosure and impact to shielding. A full spectrum energy splitter optic may be placed within the beam shroud between the BOL and BEOC to direct light towards a fiber bundle for use by IO, with little to no impact on the BEOC preliminary mechanical design.

Released 2024/05/28

Released 2024/05/28

4 INSTRUMENTATION AND CONTROLS

This section provides a brief overview of the BEOC subsystem Instrumentation and Controls (I&C) scheme to support the electrical power and signals, as described in Section 3.6. For more detailed information, reference the following documents:

- I&C System Requirement Specification (I&C SRS) [27]
- I&C System Design Specification (I&C SDS) [28]
- 55.GA PID for UPP-02 [29]
- 55.GA PID for UPP-08 [30]
- 55.GA PID for UPP-11 [31]
- 55.GA PID for UPP-14 [32]
- 55.GA PID for UPP-17 [33]

Actuators and sensors will reside within the shielded enclosure, at the required points of contact, but all drivers, controllers, and data acquisition/processing systems will be located in reserved electrical cubicles in the Diagnostic Hall. Locating the aforementioned equipment in the Diagnostic Hall mitigates environmental concerns (i.e., radiation, electromagnetic, thermal).

The BEOC subsystem instrumentation includes the following:

- Position-sensing limit switches for the actuated filter wheels and visible camera focus assemblies.
- Temperature sensing thermocouples for critical sapphire optics and optical bench assemblies.

Limit switches detect “home” and “away” positions for each filter wheel position one. Two limit switches integrated into the visible camera linear stages identify min and max travel range.

One thermocouple is required for A70-W1, A70-S1, and CAL-S1 to monitor the sapphire optic temperature. Sapphire crystal material heat absorption could contribute to background noise, causing error in measurement if substrate temperature is not known. Groupings of thermocouples on the optical benches and structures will be used to detect temperature gradients within the BEOC.

Released 2024/05/28

Released 2024/05/28

5 REFERENCES

[1] System Design Description (SDD) for 55.GA for Installation in UP2, 8, 11, and 14 (UWAVS-35), 304243-R00017, Rev A.

[2] ITER Coordinate Systems, ITER_D_2A9PXZ, v3.7.

[3] P. Yoder, Jr., Mounting Optic in Optical Instruments, 2nd ed., Bellingham, Washington: SPIE, 2008.

[4] P. Yoder, Jr. and D. Vukobratovich, Opto-Mechanical Systems Design, Design and Analysis of Opto-Mechanical Assemblies, Fourth Ed., CRC Press, 2015.

[5] Sherolinder Kinematic Mount, http://www.g2-engineering.com/products-SPH, 2017.

[6] Allectra, "363-Switch-Rad-1 Datasheet," [Online]. Available: n.a.. [Accessed 20 February 2024].

[7] 55.GA PA Annex B, ITER_D_3UT2WX, v2.8.

[8] Empire Magnetics Inc., "Radiation Hardened Stepper Motors 17 Family Size - U Series," [Online]. Available: https://www.empiremagnetics.com/prod_radiation-hardened/prod_rad_stepper_frame17.htm. [Accessed 20 February 2024].

[9] Cobalt Content in Radiation Hardened Motors, 304293-M00018, Rev A.

[10] Meeting Minute – Bertin Visit to GA – 25-29 September 2023, 304243-M00009, Rev A.

[11] "Newport Microlock," Newport, [Online]. Available: https://www.newport.com/medias/sys_master/images/images/ha8/h05/8797209034782/Microlocks.pdf. [Accessed 12 03 2024].

[12] System Design Description of Ex-vessel components, ITER_D_2YXD7E, v1.1, pp. 56-69.

[13] IS-55.GA-55.U2-001 Physical and Functional Interfaces between VisIr. And Diagnostics Upper Port UPP#2, ITER_D_X5W4BE, v1.2.

[14] IS-55.GA-55.U8-001 Physical and Functional Interfaces between VisIr. And Diagnostics Upper Port UPP#8, ITER_D_X838G5, v1.2.

[15] IS-55.GA-55.UB-001 Physical and Functional Interfaces between VisIr. And Diagnostics Upper Port #11, ITER_D_XWR3MD, v0.0.

[16] IS-55.GA-55.UE-001 Physical and Functional Interfaces between VisIr. And Diagnostics Upper Port UPP#14, ITER_D_X8XM6S.

[17] System Design Description for Interspace Support Structure (ISS), Port Cell Support Structure (PCSS) for Lower, Equatorial and Upper Ports, ITER_D_7M5RVG, v1.2.

[18] "Nelson Stud Welding & Fastening," Stanley Engineered Fastening, 2023. [Online]. Available: https://www.stanleyengineeredfastening.com/en/brands/Nelson. [Accessed 21 Febraury 2024].

[19] Nord-Lock Group, "Nord-Lock Original Washers," [Online]. Available: https://www.nord-lock.com/en-us/nord-lock/products/washers/. [Accessed 20 February 2024].

[20] Staubli, "COMBITAC MODULAR CONNECTOR SYSTEMS," [Online]. Available: https://www.staubli.com/global/en/electrical-connectors/products/modular-connector-combitac.html#tabs-a8b81c368f-item-1e5f6f9c02-tab. [Accessed 20 February 2024].

[21] Glenair, "Nuclear-Grade Connectors and Accessories," [Online]. Available: https://www.glenair.com/nuclear-grade-connectors-and-accessories/index.htm. [Accessed 20 February 2024].

Released 2024/05/28

Released 2024/05/28

[22 55-GA-A0 IR Cameras: VIS/IR (Upper) UPP02 Cabling, ITER_D_3QQP6T, v2.2.
]
[23 55-GA-B0 IR Cameras: VIS/IR (Upper) UPP08 Cabling, ITER_D_3QSJ6B, v2.4.
]
[24 55-GA-C0 IR Cameras: VIS/IR (Upper) UPP11 Cabling, ITER_D_596WA5, v2.0.
]
[25 55-GA-D0 IR Cameras: VIS/IR (Upper) UPP14 Cabling, ITER_D_3QSD6R, v2.0.
]
[26 55.GA UWAVS Bioshield Optical Labyrinth Technical Design Description, 304243-R00027.
]
[27 I&C System Requirement Specification (I&C SRS), 304243-S00024.
]
[28 I&C System Design Specification (I&C SDS), 304243-S00025.
]
[29 55-GA-A0 IR Cameras: VIS/IR TV (Upper) UPP02 PID, ITER_D_PJ4JFG, v2.0.
]
[30 55-GA-B0 IR Cameras: VIS/IR TV (Upper) UPP08 PID, ITER_D_PJAC7P, v1.0.
]
[31 55-GA-C0 IR Cameras: VIS/IR TV (Upper) UPP11 PID, ITER_D_PJCAT5, v1.0.
]
[32 55-GA-D0 IR Cameras: VIS/IR TV (Upper) UPP14 PID, ITER_D_PHUE63, v1.0.
]
[33 55-GA-E0 IR Cameras: Vis/IR TV (Upper) UPP17 PID, ITER_D_PJB95T, v3.0.
]

Released 2024/05/28

Released 2024/05/28

APPENDIX A
OPTIC LOAD AND STRESS CALCULATIONS

The equations below for optical stresses are derived in references [3] and [4].

$$A_{CSPH} = \pi r_c^2$$

$$r_c = 0.721\left(\frac{P_i K_2}{K_1}\right)^{1/3}$$

$$\sigma_{AVG} = \frac{P_i}{A_{CSPH}}$$

$$K_1 = \frac{(D_1 + D_2)}{(D_1 D_2)} \text{ for a convex optical surface}$$

$$K_1 = \frac{(D_1 - D_2)}{(D_1 D_2)} \text{ for a concave optical surface}$$

$$K_1 = \frac{1}{D_2} \text{ for a flat optical surface}$$

$$K_2 = K_G + K_M = \left[\frac{(1-\upsilon_G^2)}{E_G}\right] + \left[\frac{(1-\upsilon_M^2)}{E_M}\right]$$

$$\sigma_{CSPH} = 0.918\left(\frac{K_2^2 P_i}{R_{CyL}^2}\right)^{1/3}$$

$$S_T = (1 - 2\upsilon_G)(S_C)/3$$

$$\sigma_{C\,CYL} = 0.798\left[\frac{P_i K_1}{K_2}\right]^{1/2}$$

$$\Delta y = 1.600\left(\frac{K_2 p_i}{K_1}\right)^{1/2}$$

$$A_{C\,CYL} = bA_{C\,CYL}$$

$$\sigma_{C\,AVG} = \frac{p_i}{A_{CCYL}}$$

where
$P_i = P/N$ is the preload per spring
N is the number of springs
D_1 is twice the radius of curvature r_1 of the optical surface
D_2 is twice the radius of curvature r_2 of the contacting mechanical surface
E_G, E_M, υ_G, and υ_M are Young's modulus and Poisson's ratios for the glass and metal, respectively (see Figure 11.14)

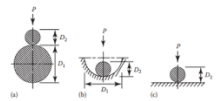

FIGURE 11.14
Key dimensions related to point contacts between elastic bodies. Shown are convex spherical pads touching (a) a convex optic, (b) a concave optic, and (c) a flat optic. The force P represents the preload. (From Yoder, P.R.,

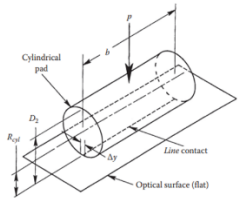

FIGURE 11.17
Analytical model for the interface between a cylindrical pad with contact length b and radius R_{CYL} and a flat optical surface. The parameter "p" is the preload per unit length of contact.

TABLE 11.4
Representative Weibull Parameters for Optical Materials

Material	Weibull Modulus m	Scale Factor σ_0 (MPa)	Test Area A (mm²)	Surface Flaw Depth s (μm)
Schott Zerodur	16.0	108.0	113	38 (SiC 600)
Schott Zerodur	5.3	293.8	113	Polished
Corning fused silica	9.89	110*	100	Polished
Schott BK-7	30.4	70.6	113	38 (SiC 600)
Schott F-2	25.0	57.1	113	38 (SiC 600)
Multispectral ZnS	9.99	77.5*	100	Polished
CVD ZnS	15.7	54.8*	100	Polished
Single crystal silicon	4.54	346.5	—	Polished
Germanium	3.4	119.8	—	Polished
Calcium fluoride	6.47	67.2*	100	Polished
Sapphire (r-plane)	4.10	545*	100	Polished to 80-50
Oxyfluoride glass (OFG)	3.71	119*	100	Polished to 10 Å rms
Spinel	19.5	248*	100	—

Source: Vukobratovich (2014).
* Characteristic strength per Equation 11.18.

$$P_f = 1 - \exp\left[-\left(\frac{\sigma}{\sigma_0}\right)^m\right] \quad (11.14)$$

Weibull equation with Weibull scale factor σ_o

$$P_f = 1 - e^{-\left(\frac{A_e}{A_o}\right)\left(\frac{\sigma}{\sigma_0}\right)^m} \quad (2)$$

Effective area for ring-on-ring test

$$A_e = 2\pi a^2\left\{\frac{44(1+\nu)}{3(1+m)}\frac{5+m}{2+m}\left(\frac{b-a}{bc}\right)^2\left[\frac{2c^2(1+\nu)+(b-a)^2(1-\nu)}{(3+\nu)(1+3\nu)}\right]\right\} \quad (6)$$

Effective area for pressure-on-ring geometry

$$A_e \approx \frac{4\pi(1+\nu)}{1+m}\left(\frac{b}{c}\right)^2\left[\frac{2c^2(1+\nu)+b^2(1-\nu)}{(3+\nu)(1+3\nu)}\right] \quad (7)$$

$$\Delta = (K_A - K_B)\left(\frac{P}{t^3}\right)$$

$$K_A = \frac{(3)(m^2-1)[a^4 - b^4 - (4)(a^2)(b^2)\ln(a/b)]}{[(4)(\pi)(m^2)(E_M)(a^2)]}$$

$$K_B = \frac{(3)(m^2-1)(m+1)[(2)\ln(a/b) + (b^2/a^2) - 1][b^4 + (2)(a^2)(b^2)\ln(a/b) - (a^2)(b^2)]}{(4)(\pi)(m^2)(E_M)[(b^2)(m+1) + (a^2)(m-1)]}$$

$$S_B = \frac{K_C P}{t^2} = \frac{S_Y}{f_S}$$

$$K_C = \left[\frac{3}{2\pi}\right]\left[1 - \frac{2mb^2 - 2b^2(m+1)\ln(a/b)}{a^2(m-1) + b^2(m+1)}\right]$$

P is the total preload
t is the thickness of the cantilevered section of the flange
a is the outer radius of the cantilevered section
b is the inner radius of the cantilevered section
m is the reciprocal of Poisson's ratio (ν_m) of the flange material
E_M is Young's modulus of the flange material

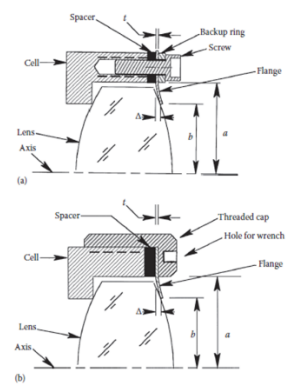

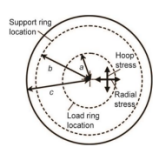

Load radius = a = 0.80 cm
Support radius = b = 1.60 cm
Disk radius = c = 1.90 cm
Disk thickness = h = 0.20 cm
Poisson's ratio = ν = 0.30

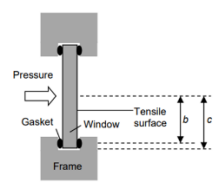

FIGURE 2. Geometry of Ring-on-Ring Flexure Test of a Polished Ceramic Disk.

Opto-Mechanical Systems Design, Volume 1_Design and Analysis of Opto-Mechanical Assemblies (PDFDrive).pdf

Released 2024/05/28

Released 2024/05/28

APPENDIX B
STEPPER MOTOR OPERATION CALCULATIONS

Description: VIS Filter wheel gear calculations
Notes: Determine torque/speed required to rotate one filter wheel
Last updated: 2023.07.10

Gear module	1.0		
Gear specifications			Notes
d_1	30	mm	Input gear pitch diameter
N_1	30		Input gear Qty teeth
d_2	280	mm	Output gear pitch diameter
N_2	280		Output gear Qty teeth
Filter wheel specifications			Notes
Wheel mass	1.32	kg	From CAD - 2023.07.10
Fric. Coeff.	0.002		Deep groove ball bearing
FoS	1.5		Factor of Safety
Force	0.039	N	Req. force to rotate filter wheel.
Torque	0.583	N-mm	Input gear torque required to rotate wheel
	0.083	oz-in	"
Rotation speed calculations			Notes
n-filters	6		Number of filters / wheel
θ-filter	60	deg	Angle between filters
	1.05	rad	"
t-filter change	0.50	s	Time to switch to adjacent filter
ω_2	2.09	rad/s	Filter wheel angular velocity = θ/t
n_2	0.33	rev/s	Filter wheel rotation speed = rad/2π
n_1	3.11	rev/s	Input gear rotation speed = $n_2*(d_2/d_1)$

Released 2024/05/28

Released 2024/05/28

APPENDIX C
MATERIAL SUMMARY

Table 5. Material Specification Table

Component	Material
Stainless steel shielding and structure	SS316L
Cadmium shielding	Cadmium (Cd)
Iron shielding	Pure Iron (Fe)
Neutronic shielding	Boron Carbide (B4C)
PCSS Interface Plate	A286 Stainless Steel
Pucks – Interface Plate	Inconel 718
Optical bench skins and honeycomb core	SS316L
Optical bench pedestals and supports	SS316L
Mirror cells and bases	AL 6061-T6
Lens barrels and bases	SS316L
Optical lenses and mirrors	Glass (optical)
Optical windows	Sapphire (optical)
Kinematic mechanism (cone, sphere/cylinder, v-groove)	SS430
Filter wheel housing	AL 6061-T6
Filter wheel gears	SS316L
Structural fasteners	Class 10.9 Carbon Steel
Stepper motors	Stainless steel, Samarium Cobalt magnet
Linear stage	Aluminum housing, stainless steel drive train
IR cameras	TBC at FDR
VIS cameras	TBC at FDR
IR calibration source	Stainless steel (cabinet) SALI-2 (insulation) Carbon/Ceramic (heated cavity)
VIS calibration source	TBC at FDR

Released 2024/05/28

Released 2024/05/28

Released 2024/05/28

Released 2024/05/28

GENERAL ATOMICS